PL-TR--95-2128
Environmental Research Papers, No. 1178

CRRESELE DOCUMENTATION

Donald H. Brautigam
Jabin T. Bell, 1Lt, USAF

31 July 1995

PHILLIPS LABORATORY
Directorate of Geophysics
AIR FORCE MATERIEL COMMAND
HANSCOM AIR FORCE BASE, MA 01731-3010

"This technical report has been reviewed and is approved for publication"

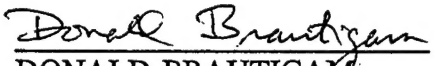

DONALD BRAUTIGAM
Space Particles Env. Branch
Space Physics Division

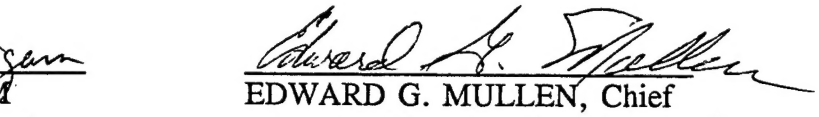

EDWARD G. MULLEN, Chief
Space Particles Env. Branch
Space Physics Division

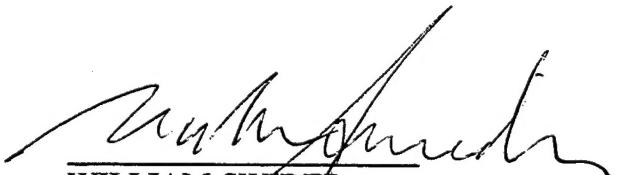

WILLIAM SWIDER
Deputy Director
Space Physics Division

This report has been reviewed by the ESC Public Affairs Office (PA) and is releasable to the National Technical Information Service (NTIS).

Qualified requestors may obtain additional copies from the Defense Technical Information Center. All others should apply to the National Technical Information Service.

If your address has changed, or if you wish to be removed from the mailing list, or if the addressee is no longer employed by your organization, please notify PL/TSI, 29 Randolph Road, Hanscom AFB, MA 01731-3010. This will assist us in maintaining a current mailing list.

Do not return copies of this report unless contractual obligations or notices on a specific document requires that it be returned.

REPORT DOCUMENTATION PAGE

Form Approved
OMB No. 0704-0188

1. AGENCY USE ONLY *(Leave blank)*	2. REPORT DATE	3. REPORT TYPE AND DATES COVERED
	31 July 1995	Scientific, Interim

4. TITLE AND SUBTITLE

CRRESELE Documentation

5. FUNDING NUMBERS

PE 62601F
Proj: 7601
Task: 22
Work Unit: 03

6. AUTHOR(S)

Donald H. Brautigam, Jabin T. Bell, 1st Lt, USAF

7. PERFORMING ORGANIZATION NAME(S) AND ADDRESS(ES)

Phillips Laboratory/GPSP
29 Randolph Road
Hanscom AFB, MA 01731-3010

8. PERFORMING ORGANIZATION REPORT NUMBER

PL-TR-95-2128
ERP, No. 1178

9. SPONSORING/MONITORING AGENCY NAME(S) AND ADDRESS(ES)

10. SPONSORING/MONITORING AGENCY REPORT NUMBER

11. SUPPLEMENTARY NOTES

12a. DISTRIBUTION/AVAILABILITY STATEMENT

Approved for public release;
Distribution unlimited

12b. DISTRIBUTION CODE

13. ABSTRACT *(Maximum 200 words)*

This technical report documents the software package CRRESELE developed by the Space Physics Division of the Phillips Laboratory. CRRESELE utilizes electron radiation belt models constructed from data measured by the High Energy Electron Fluxmeter (HEEF) flown on the Combined Release and Radiation Effects Satellite (CRRES). CRRES flew in a geosynchronous transfer orbit for 14 months during solar maximum. The electron models are omnidirectional flux maps binned in L shell and B/B_0 (azimuthal symmetry is assumed) for a given energy. The CRRESELE utility calculates electron omnidirectional fluences (differential and integral) for 10 energy intervals (0.5-6.60 MeV). A user-specified orbit is traced through eight different outer zone electron flux models, at each energy, to provide an extimate of electron fluences received by a satellite under a wide range of magnetospheric conditions. Six of the eight CRRESELE models are parameterized by geomagnetic activity, the seventh is simply a mission average, and the eighth is constructed from maximum flux values. caution must be used when interpreting the results because CRRESELE is restricted to modeling the outer zone electrons from L=2.5-6.5, and consequently, excludes any electron fluence contributions from the inner zone and slot region.

14. SUBJECT TERMS

CRRES, Radiation belts, Electron, Fluence

15. NUMBER OF PAGES

62

16. PRICE CODE

17. SECURITY CLASSIFICATION OF REPORT	18. SECURITY CLASSIFICATION OF THIS PAGE	19. SECURITY CLASSIFICATION OF ABSTRACT	20. LIMITATION OF ABSTRACT
Unclassified	Unclassified	Unclassified	SAR

Contents

Illustrations

Tables

Acknowledgements

Many people contributed to the success of the High Energy Electron Fluxmeter (HEEF) and the creation of CRRESELE. E.G. Mullen headed the CRRES/SPACERAD team and has insisted on user-friendly data products. CRRESELE and its sister utilities, CRRESRAD and CRRESPRO, have benefited greatly from his guidance. HEEF was designed and assembled by Panametrics. Fred Hanser and Bronek Dichter of Panametrics, Ernest Holeman and Dan Madden of Boston College, and Don Brautigam and Robb Frederickson of Phillips Lab, were instrumental in the postflight data analysis. Don Brautigam designed and constructed the CRRESELE electron models. Carl Hein and Jim Bass of RADEX developed routines for mapping equatorial data down the field lines, and modified LOKANGL to run on the IBM PC. The Olson-Pfitzer Static and the IGRF85 magnetic field models were modified to run on the IBM PC by K.A. Pfitzer of McDonnell Douglas Space Systems Corporation. The CRRESRAD software, on which CRRESPRO and CRRESELE is based, was written by Kevin Kerns. Jabin Bell modified CRRESRAD to produce CRRESELE. Portions of this document describing the mechanics of running the utility program, particularly the Appendices, remain largely untouched from their original form appearing in the CRRESRAD documentation written by Kevin Kerns and M.S. Gussenhoven.

CRRESELE Documentation[1]

1. OVERVIEW

For a user-specified orbit, the CRRESELE software utility determines yearly omnidirectional fluences (both differential and integral) for ten energy intervals from 0.50 to 6.60 MeV. CRRESELE determines these fluences for each of eight outer radiation belt electron models created from data obtained by the High Energy Electron Fluxmeter (HEEF) flown on the Combined Release and Radiation Effects Satellite (CRRES). Six of the eight CRRESELE models are parameterized by the geomagnetic activity index Ap. In addition to these six models (CRRES_Ap), there are two extra models. One is the average over the entire mission (CRRES_AVE), and the second, a 'worst case' model, is constructed from the mission's maximum fluxes (CRRES_MAX). CRRES was launched on 25 July 1990 into a geosynchronous transfer orbit with an inclination of 18°, a perigee of 350 km, an apogee of 33000 km, and an orbital period of 9 hours 52 minutes. It returned data for approximately 14 months during solar maximum, traversing the radiation belts twice per orbit, until it lost power on 12 October 1991.

Preliminary CRRES electron models published previously (Brautigam, et al., 1992) were constructed from spin-averaged data which eliminated the pitch angle information required for projecting the fluxes along the magnetic field line. The preliminary models are therefore inappropriate for use in the CRRESELE utility which requires that an omnidirectional flux be defined all along a field line. The revised electron models described in this document have been constructed using the full pitch angle distribution, and the spatial resolution has been increased from the preliminary models as well (decreasing the L bin width from 0.2 to 0.05 R_E). Furthermore, calibration data resulting from post-launch analyses, which were not available at the time the preliminary models were constructed, have been used in

Received for publication 31 July 1995

processing the data for the current models.

The CRRES electron models presented here are limited to the outer zone electron belts in the region of $2.5 \leq L \leq 6.55$ for reasons explained in Section 4. Caution must therefore be exercised when interpreting CRRESELE's yearly fluences because all electron fluence contributions from the inner zone and 'slot' region (between the inner and outer zone) have been excluded.

Section 2 discusses a minimum of magnetospheric concepts and terminology required to understand the construction of the electron models. The geomagnetic activity index defined and used in the construction of the electron models is explained in Section 3. Details of the HEEF instrument design, calibration, and data corrections are included in Section 4. The construction of the omnidirectional flux models used in CRRESELE is outlined in Section 5, and the calculation of orbital fluences is described in Section 6. Section 7 describes the logical flow and interface of the CRRESELE software package. Finally, Appendices A-G cover in greater detail certain topics only touched upon in the main text. Appendix H includes the CRRESELE model equatorial flux vs L profiles.

2. MAGNETOSPHERIC CONCEPTS AND TERMINOLOGY

The Earth's radiation belts are comprised of charged particles of sufficient energy (>200 KeV) that the effect of the convection electric field on their trajectories is negligible; and they are thus controlled predominantly by the Earth's magnetic field. A radiation belt particle therefore exhibits three approximately periodic motions while moving through the geomagnetic field: a gyration about the magnetic field, a bounce motion along the field line (reversing direction at its mirroring point in the northern and southern hemisphere), and an azimuthal drift motion about the Earth due to the magnetic field gradient and field line curvature. Averaged over its gyro-motion, the surface a particle follows during its drift motion is referred to as its "drift shell." Because of the extent to which these particles are constrained by the Earth's magnetic field, it is advantageous to specify their position by two magnetic field parameters. The first magnetic field parameter is the McIlwain L parameter (McIlwain, 1961), which is referred to hereafter as simply "L". In a dipole magnetic field, the L of a given point in space is the equatorial radial distance in Earth radii (R_E) of the field line passing through that point. The Earth's magnetic field has some non-dipole components, and L is calculated by determining which dipole field line the actual field line would correspond to if the Earth's magnetic field were relaxed to a dipole field. The second magnetic field parameter is B/B_0, the ratio of the magnetic field magnitude at a given point along a field line to the minimum magnetic field magnitude along the same field line. The magnetic field is strongest near the poles and weakest near the equator so that B/B_0 equals 1.0 near the equator and

increases towards the magnetic poles. For a dipole field, B/B_0 is a function only of magnetic latitude and is equal to 1 on the magnetic equator. The solid lines in Figure 1 are field lines of L = 2, 3, 4, 5, and 6 of a dipole magnetic field centered in Earth. The dotted lines show constant B/B_0 contours in an Earth-centered dipole field between -40° and +40° (10° intervals) magnetic latitude.

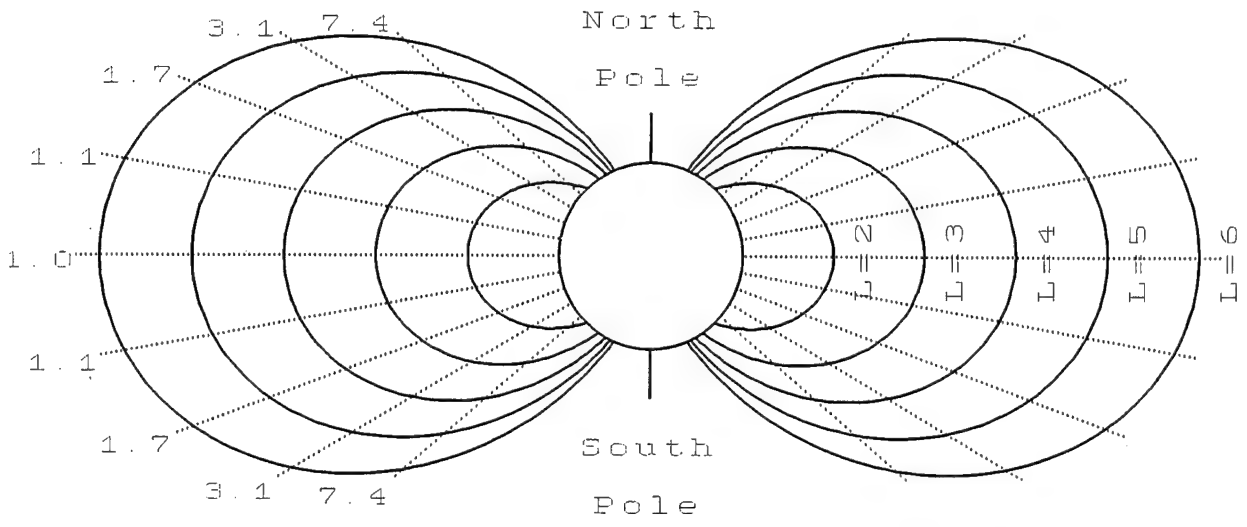

Figure 1. L Shells 2, 3, 4, 5, and 6 (Solid Lines) and Lines of Constant B/B_0 = 1.0, 1.1, 1.7, 3.1, and 7.4 (Dashed Lines) in a Dipole Field Centered in Earth.

The Olson-Pfitzer static external magnetic field model and the IGRF85 internal magnetic field model were used in the calculation of the L and B/B_0 values used to bin the CRRES flux data. The IGRF85 model specifies the magnetic field caused by currents inside Earth (IAGA Division I, Working Group 1, 1986). This field is nearly dipolar with an 11.5° tilt and 436 km offset with respect to Earth's spin axis and is slowly changing with time (Knecht and Shuman, 1985). The IGRF model accounts for the slow time variation of the field as well as the tilt and non-dipole contributions to the field. The Olson-Pfitzer static magnetic field (Olson and Pfitzer, 1974) models the external contributions to the Earth's total magnetic field from the magnetopause current, the ring current, and the magnetosphere tail current. The model also accounts for the tilt of Earth's dipole with respect to the Earth-Sun line. The external currents that contribute to the magnetic field change with variations in the solar wind and magnetospheric activity. However, the static external model used here assumes these currents do not change and uses values from average quiet conditions.

As a particle travels along a magnetic field line, its direction relative to the field line is specified by its pitch angle, $\alpha = \sin^{-1}(p_\perp/p_\parallel)$, where $p_\perp$ and $p_\parallel$ are the particle's momentum (p) components

perpendicular and parallel to the magnetic field. A pitch angle distribution (PAD) is defined as the distribution of particle flux vs pitch angle for a fixed energy. Assuming that the magnetic field does not change appreciably on the time scale of the particle's gyration period, then the particle's magnetic moment ($\mu = p^2 \sin^2\alpha / 2mB$, typically identified as the *first adiabatic invariant*) is conserved during the particle's bounce motion along the magnetic field line. Under such conditions, the particle's pitch angle at the magnetic equator (α_o), where the magnetic field is given by B_o, is related to its pitch angle at any other point along the same field line (α), where the magnetic field is given by B, by the following expression: $\sin^2\alpha_o / B_o = \sin^2\alpha / B$. Given a pitch angle distribution on the magnetic equator, the pitch angle distribution may be determined at any other point along the field line. This result is used to construct the final flux models as discussed in Section 5. Chapter 5 of the *Handbook of Geophysics and the Space Environment* (Spjeldvik and Rothwell, 1985) contains a more complete description of Earth's magnetosphere and radiation belts.

3. GEOMAGNETIC ACTIVITY INDEX, Ap_{15}

To monitor geomagnetic disturbances caused by variations in the solar wind pressure and magnetospheric currents, a network of ground station magnetometers exists around the world. There are numerous magnetic activity indices derived from these ground level magnetic field data. The "K" index is related to the maximum deviation of the magnetic field's horizontal component (over a 3 hour period) from an established quiet time baseline at an individual station. It is defined on a quasi-logarithmic scale. The "Ap" index is essentially a daily average created from eight 3-hr K indices (converted to a linear scale) from a network of 13 magnetic observatories between the geomagnetic latitudes of 46° and 63°, and is produced by the Geophysics Institute at Gottingen, Germany (SESC, 1988). This daily index (Ap) is archived in NOAA's monthly publication *Solar-Geophysical Data prompt reports*. However, as quoted from SESC's *Glossary of Solar-Terrestrial Terms*: "for daily operational uses (since several weeks are required to collect the data and calculate the index), Air Force Global Weather Central estimates the value of the Ap index by measuring the geomagnetic field in near-real time at several Western Hemisphere magnetometer stations and statistically weighting the data to represent the Gottingen Ap." (SESC, 1988) This estimated daily planetary A index ($\sim$Ap) is published in NOAA's *Preliminary Report and Forecast of Solar Geophysical Data*.

For the purpose of constructing the CRRES_Ap models (Section 5), we define a new index derived from the Ap index. For a given day, the preceding 15 daily values of Ap are averaged to form the Ap_{15} index. The Ap_{15} index may be derived from either the estimated or archived Ap values; the results agree

within ± 20 percent and display the same qualitative variations. A linear regression was performed on 455 days of estimated and archived indices and yielded the following linear relation:

$$\mathbf{Ap_{15}(estimated) = 0.8 \cdot Ap_{15}(archived) + 2.6},$$

with a correlation coefficient of 0.99. When Ap_{15} is referred to in this document, it is assumed that it is derived either directly from the weekly estimated Ap or indirectly (via the above linear relation) from the archived version of Ap.

Although CRRES did not sample as large a fraction of a solar cycle as was hoped for (due to a premature battery failure), it did return data during a time period when the magnetosphere exhibited a wide range of magnetic activity. Plotted in Figure 2 is the Ap_{15} index for 12 years (1/1/80 - 12/31/91). Solar minimum occurred in 6/86 and solar maximum in 8/90. The time interval for which CRRES returned data is marked for comparison with the full solar cycle. Considering the 12 years of Ap_{15} shown here, the timing of the CRRES mission was fortuitous in that it permitted observation of the radiation belts during a period including both the magnetosphere's weakest and strongest geomagnetic activity.

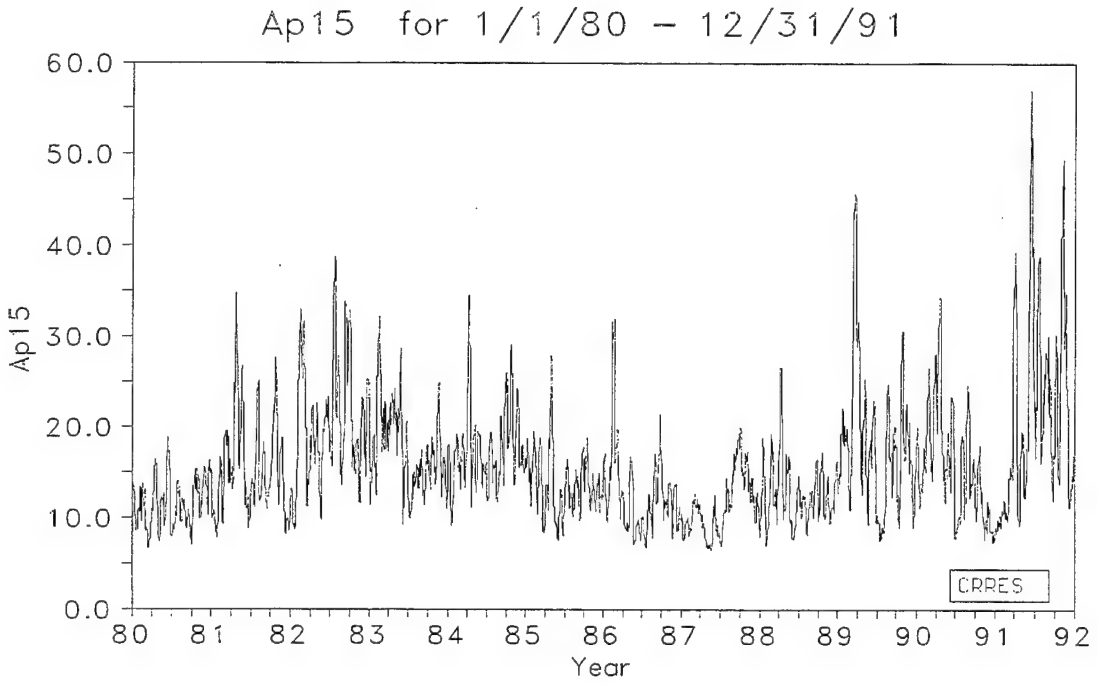

Figure 2. Ap_{15}, plotted for 1980-1992, is derived from the daily Ap index published in the monthly *Solar-Geophysical Data Prompt Reports*. The CRRES epoch is designated on the far right.

4. HEEF INSTRUMENT

The flux models used by CRRESELE are based on *in situ* flux measurements made by CRRES's High Energy Electron Fluxmeter (HEEF). HEEF was designed to measure the flux of 1-10 MeV electrons in 10 differential number flux channels and to return a complete spectrum every 0.512 seconds. The telescope consists of a well collimated stack of three particle detection elements; the top two being solid state detectors, and the third, a bismuth germanate (BGO) crystal. A passive beryllium shield is placed at the entrance of the telescope to stop lower energy (< 0.3 MeV) electrons. A plastic scintillator surrounds the BGO crystal to veto particles that penetrate it from the sides and would otherwise trigger accidental counts. A detailed description of HEEF design (Hunerwadel, et al., 1987) and pre-flight calibration results (Dichter and Hanser, 1989) are available. As a result of post-launch satellite developments, HEEF was forced to operate far below design temperature specifications. This colder environment dramatically reduced the BGO crystal's counting efficiency and prompted experimentation with HEEF's replica ($HEEF_2$). Algorithms were developed to adjust the geometric factors and channel energies for the temperature dependencies (Dichter and Hanser, 1991; Dichter and Hanser, 1992). It was also found that the count rates in the front solid state detectors were severely limited during intervals of intense low energy (100's of keV) electron fluxes, affecting count rates in the primary differential channels. This problem prompted further investigation into the response of $HEEF_2$ solid state detectors to intense low energy electrons, and led to a set of correction algorithms to be applied to the original flight data (Hanser, 1995). As the result of extensive post-launch analysis of the actual flight data and $HEEF_2$ test data, the spectrum energies were revised. The lowest energy differential channel was omitted because of the large uncertainty in its geometric factor, and the highest energy differential channel was omitted because its counting efficiency was so low that it rendered little statistically meaningful data for modelling purposes. One fringe benefit from the post-launch calibration work was the information required to derive two extra lower energy (0.65 and 0.95 MeV) differential flux channels from the two solid state detectors. The final set of energy channels is provided in Section 5 as Table 1.

5. ELECTRON FLUX MODELS

The CRRES mission survey plot for 1.60 MeV electron flux is shown in the top panel of Figure 3. The flux intensity is gray-scale coded, with black the most intense. L is along the y-axis and orbit number is along the x-axis. A vertical slice is the electron flux profile for a given orbit (average of

ascending and descending leg). Evident in this survey of flux profiles are the three distinct regions of the electron radiation belts. The exact boundaries of these regions are loosely defined, and are dependent on electron energy and magnetic activity. The interval L=1.25-1.75 spans the inner electron belt, and is the most stable region. The 'slot' region, found between L=1.75 to 2.5, is typically void of MeV electrons. The interval $L \geq 2.5$ spans the outer electron belt, and is periodically punctuated by large enhancements in flux. On 24 March 1991, a magnetic storm caused a sudden but prolonged reconfiguration of the inner magnetosphere, with the relatively rare formation of an additional electron belt (Blake, et al., 1992) and proton belt (Mullen, et al., 1991). As seen in the survey plot, this storm introduced a new population of MeV electrons into the 'slot' region. It was determined that the energy peak of the new electron belt was greater than 15 MeV (Blake, et al., 1992) which is beyond HEEF's energy range.

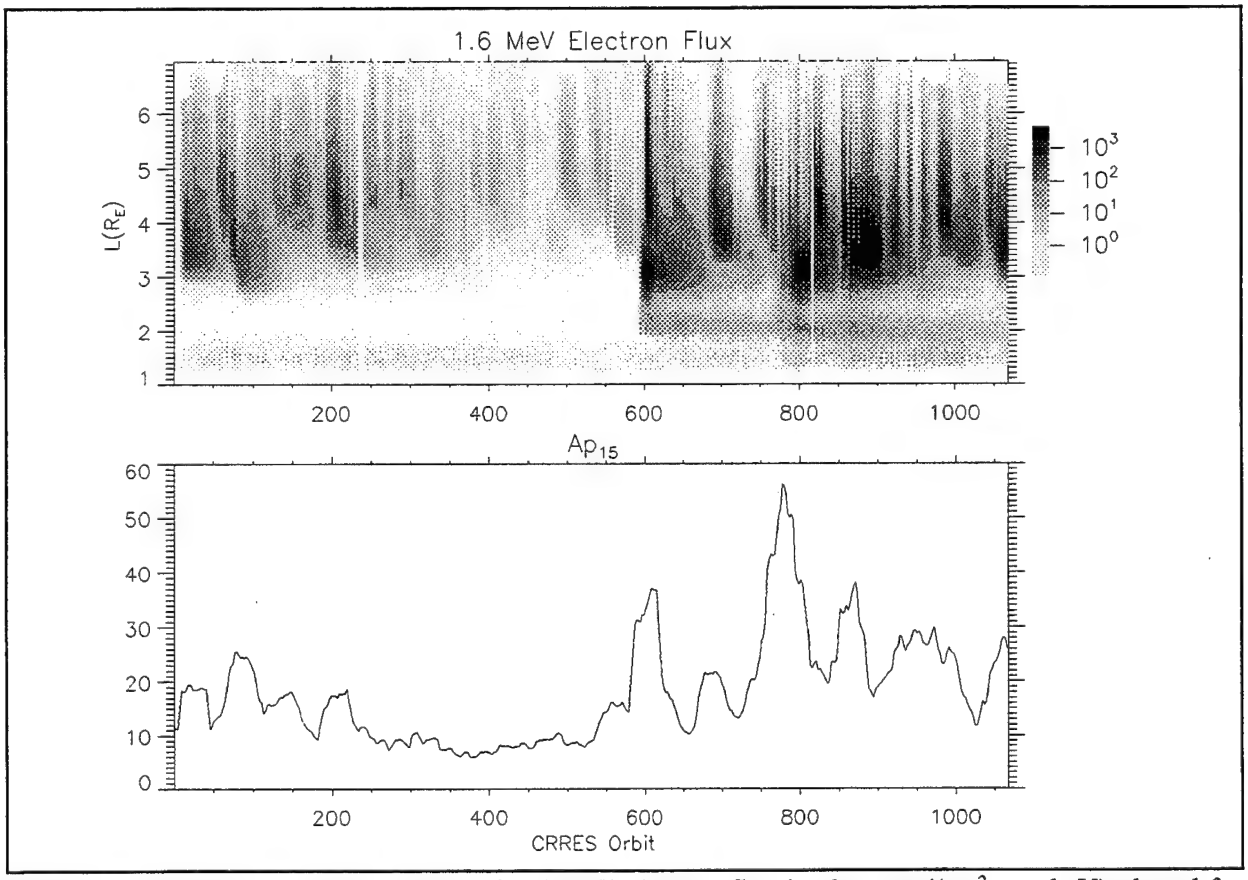

Figure 3. Top panel is mission survey of 1.6 MeV electron flux in electrons/(cm^2 s sr keV) plotted for L shell versus orbit number. Bottom panel is Ap_{15} over the same time period.

The potential problem of energetic proton contamination of HEEF in the inner zone has not been assessed at this time. The 'slot' region, populated by the temporary third electron belt during the second half of the CRRES mission, would require special treatment than that for the outer zone belt. Therefore,

the CRRES electron models presented here are developed for the outer zone electron belts only, limited to the interval $2.5 \leq L \leq 6.55$. Caution must therefore be exercised when interpreting the yearly fluences calculated by CRRESELE because any electron fluence contributions from the inner zone or slot region have been intentionally excluded.

The construction of the CRRES electron models is a long, involved process which is briefly discussed here and outlined in greater detail in Appendix G. The 0.512-second count rates are first binned by L (0.05 R_E wide bins) and pitch angle (5° wide bins), folding the pitch angles > 90° into the 0°-90° quadrant. Various correction algorithms are next applied to these average count rates, which are then converted to average fluxes. For a given energy and L, the bin average pitch angle distributions are mapped to the magnetic equator. A database of daily average equatorial fluxes binned by day, energy, pitch angle, and L ($2.5 \leq L \leq 6.55$) is then created. This database is next sorted into eight models as described below.

Six of the eight models are parameterized by geomagnetic activity. The Ap_{15} index described in Section 3 is determined for each day of the CRRES mission using NOAA's weekly published values of the estimated daily planetary index ($\sim$Ap) (SESC, 1990-1991). This Ap_{15} index is plotted as the bottom panel of Figure 3. The lowest Ap_{15} values represent very quiet magnetospheric conditions, during which one can expect to find lower fluxes peaking at higher L's. Likewise, the highest Ap_{15} values represent very active magnetospheric conditions, during which one can expect to find higher fluxes peaking at lower L's (Brautigam, et al., 1992). The first large peak ($Ap_{15} \sim 37$) after the extended quiet time corresponds to the 24 March 1991 storm. The largest peak ($Ap_{15} \sim 55$) corresponds to the extremely active period in early June 1991. The range of Ap_{15} observed during the CRRES period ($Ap_{15} = 6$ to 55) is divided into 6 intervals (5-7.5, 7.5-10, 10-15, 15-20, 20-25, 25-55). The daily average flux data base described above is then sorted according to the corresponding daily Ap_{15} value. For example, all the daily average fluxes identified with an Ap_{15} in the range 5-7.5 are averaged together to form a flux model associated with that geomagnetic activity level. This procedure results in six electron equatorial flux models (for each of 10 energies), collectively referred to as CRRES_Ap. Table 1 below summarizes the statistics of the 6 CRRES_Ap models. The first column is the model number, the second column gives the range of Ap_{15} values associated with each model, with the average value of Ap_{15} for this range given in column three. A total of 402 days of data is used in constructing these models. The fourth column gives the total number of days sorted into each of the individual models, reflecting the distribution of Ap_{15} values. The fifth column simply gives the percent of the total database used in each model (days in column 4 divided by 402 days).

Table 1. Summary of CRRES_Ap Model Separation and Statistics

Model #	Ap_{15} Range	Ave Ap_{15}	Days/Model	% of Total
0	5.0 - 7.5	6.8	13	3.2
1	7.5 - 10.	8.7	83	20.7
2	10.0 - 15.	12.5	69	17.1
3	15.0 - 20.	17.1	82	20.6
4	20. - 25.	22.4	72	17.7
5	25. - 55.	35.7	83	20.7

Two additional models (#s 6 and 7), independent of Ap_{15}, are constructed from the same daily average flux data base referred to above. For model #6 (CRRES_AVE), the entire data base is averaged together providing a mission average model. Model #7 (CRRES_MAX) is constructed from the maximum flux found at each L bin of the daily average database.

HEEF has small energy dependent geometric factors, which translate to low count rates. These low count rate statistics are most pronounced in the lower activity models, particularly for the highest energies and at the inner and outer edges of the belt. The poor statistics result in a large degree of scatter in these regimes, thus it was decided to smooth the model profiles. The procedure for this smoothing is outlined in Appendix G (step 6).

To compute the total electron fluence for an orbit of arbitrary inclination, it is necessary to first project the equatorial directional fluxes back along the field lines towards the Earth. The midpoint of each of the 81 L bins corresponds to a single magnetic field line whose length is divided into 34 different B/B_0 intervals (refer to Figure 1). The spacing of these intervals corresponds to 2° steps in magnetic latitude in a dipole magnetic field from 0°to 68°. As discussed in Section 2, this field line projection (in either direction) is accomplished using the relation implied by the conservation of the first adiabatic invariant. The equatorial flux in each L and pitch angle bin is projected along its corresponding field line to a unique B/B_0 interval. The resulting pitch angle distribution, in each spatial bin $(L,B/B_0)$, is integrated over pitch angle to give the omnidirectional flux. This transformation from a 1-dimensional $(L,B/B_0=1)$ equatorial directional flux to a 2-dimensional $(L,B/B_0 \geq 1)$ omnidirectional flux is performed for each model at each energy. The final result is 80 omnidirectional flux model files, labeled "FLUX_MOD.ij", where i denotes the model number (i=0 to 7) and j, the channel number (j=0 to 9).

Each file includes an 81 (L bin) by 34 (B/B_0 bin) dimensioned array of omnidirectional flux. The explicit data format of these files is detailed in Appendix B. The equatorial omnidirectional flux vs L profiles for the eight models (at a given energy) are provided in Appendix H.

Radiation belt dynamics are quite complex, and are far from being completely understood. Typically observed are electron variations due to abrupt injection and dropout events, as well as variations due to more gradual diffusive mechanisms. It would be naive to expect, therefore, that a single index would be capable of modeling, to a high degree of correlation, all the variations seen in the radiation belts. The spread in the daily flux profiles that were used in constructing the individual CRRESELE models is discussed in Appendix H. Also included there is a comparison between the environment inferred by the CRRES_Ap models (and the Ap_{15} database) and that as inferred by DMSP/J4 background measurements.

6. FLUENCE CALCULATIONS

The eight models are stored as differential omnidirectional flux, $J_{bin}(E)$, as a function of E (energy) and spatial bin (L, B/B_0). To obtain the desired yearly differential omnidirectional fluence, $F_{yr}(E)$, and integral omnidirectional fluence, $\mathcal{F}_{yr}(>E)$, the time spent in each spatial bin traversed by the user-specified orbit, τ_{bin}, is first determined. It is important to realize that only those spatial bins within the bounds of the models ($2.5 \leq L \leq 6.55$ and $1 \leq B/B_0 \leq 684.6$) are used in the fluence calculation. For a given spatial bin, the differential omnidirectional fluence, $F_{bin}(E)$, and integral omnidirectional fluence, $\mathcal{F}_{bin}(>E)$, are then calculated as follows:

$$F_{bin}(E_i) = J_{bin}(E_i) \cdot \tau_{bin} \quad ; \quad \mathcal{F}_{bin}(>E_j) = \sum_{i=j}^{10} F_{bin}(E_i)\,\Delta E_i$$

where E_i is the central energy ($E_{central}$), ΔE_i is the energy width of channel i, and $>E_j$ indicates the lower energy (E_{lower}) threshold for channel j; all as listed in Table 2 of this section.

To facilitate the determination of $\mathcal{F}_{bin}(>E)$, the fictitious channels 0.a and 1.a have been introduced (see Table 2) to fill the gap in the energy spectrum between channels 0 and 1, and between channels 1 and 2, respectively. The omnidirectional flux at these two fictitious channels is determined by interpolating between the adjacent channels in each case. This procedure is followed to provide a stepwise continuous spectrum, which can then be summed over a discrete set of energies (as indicated above) to give the integral omnidirectional fluence.

Table 2. Channel Energies

CH #	E_{lower} (MeV)	$E_{central}$ (MeV)	E_{upper} (MeV)	ΔE (MeV)
0	0.50	0.65	< 0.80	0.30
0.a	0.80	0.825	< 0.85	0.05
1	0.85	0.95	< 1.05	0.20
1.a	1.05	1.15	< 1.25	0.20
2	1.25	1.60	< 1.70	0.45
3	1.70	2.00	< 2.10	0.40
4	2.10	2.35	< 2.50	0.40
5	2.50	2.75	< 2.90	0.40
6	2.90	3.15	< 3.30	0.40
7	3.30	3.75	< 4.10	0.80
8	4.10	4.55	< 4.95	0.85
9	4.95	5.75	< 6.60	1.65

The final reported fluences are calculated by summing over all traversed bins (within the model bounds) and then multiplying by the appropriate time scaling factor (S) required to normalize the results to a yearly fluence:

$$F_{yr}(E_i) = S \cdot \sum F_{bin}(E_i) \quad ; \quad \mathscr{F}_{yr}(>E_j) = S \cdot \sum \mathscr{F}_{bin}(>E_j) \quad ,$$

where S = the number of days in 1 year divided by the duration of the orbit trace in days (indicated as user-input "Length" in Appendix A). The units of $F_{yr}(E)$ are electrons/(cm^2 keV) and those of $\mathscr{F}_{yr}(>E)$ are electrons/cm^2. The percent of time spent by the orbit outside the model bounds is provided in the fluence output file. It should be stressed again that the calculated fluences are from the outer zone electron belt only. A low earth polar orbit will pass within the model bounds only about 15 percent of

the time, whereas a nearly geosynchronous orbit will remain within the model bounds nearly 100 percent of the time. To assess the radiation environment accurately, one must treat this information as one piece of the puzzle, and incorporate information from other sources, such as CRRESRAD and CRRESPRO, to render a complete picture.

7. CRRESELE SOFTWARE PACKAGE

CRRESELE requires a DOS based PC computer (an 80386 at minimum) with a math coprocessor, a color VGA card, and a hard drive. A printer is not required but is useful. CRRESELE must be installed using the supplied batch file INSTALL.BAT. Install CRRESELE from the floppy disk drive. For example, if the disk is in drive A, type **A: <enter>**, and then type **INSTALL <enter>**. The directory C:\CRRESELE will be created, and CRRESELE files then installed. An ASCII README file is included with the CRRESELE software. To read this file enter **TYPE README.TXT | MORE** on the command line and press <enter>. README documents recent updates to the software and has a directory list of the files included with CRRESELE. As a precaution against viral contamination, make sure the ".EXE" files are the same size and date as given in the README file. A sample session for determining the fluence from a CRRES-like orbit is shown in Appendix A, and the sample output file is listed in Appendix F.

Figure 4 shows a flow diagram of the CRRESELE execution. The solid arrows indicate the direction of flow, and the dashed arrows indicate the input and output at each step. After each logical step, CRRESELE stops and presents the user with information about what it will be doing next, then waits for a key to be pressed before continuing.

To begin execution, type **CD C:\CRRESELE <enter>**. To begin, first time users of CRRESELE should type **CRRESELE** on the command line. The user will be queried for the name to be associated with the orbit to be evaluated. This name will be used for all of the data files subsequently created for this orbit. The data files can be written to another directory by adding the path to the name. For example, to run an orbit called "SAMPLE" and store the data in "C:\ORBITS\", specify the name as "C:\ORBITS\SAMPLE". No extension should be given in the name since default extensions are used. In Figure 4, the input name is represented by "?NAME?". If files from a previous CRRESELE-run of the same name exist, CRRESELE will ask the user if these files should be used. A second option for users familiar with CRRESELE is to include the name on the command line by typing **CRRESELE ?NAME?**. When this option is used, CRRESELE does not stop to tell the user what it is doing or wait

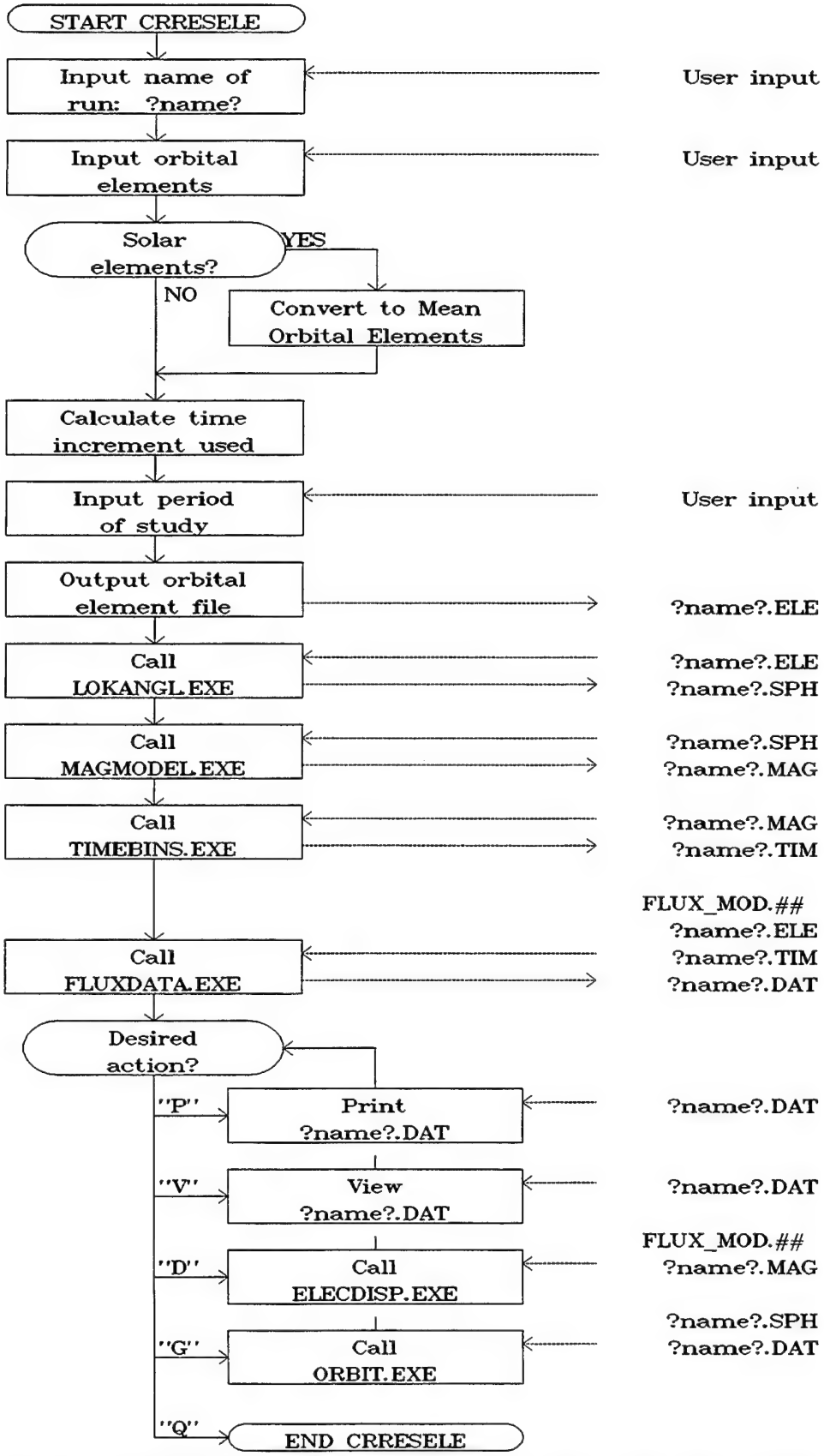

Figure 4. Simplified flow diagram of CRRESELE. Solid arrows refer to logical flow, and dashed arrows refer to input/output.

for user input. This allows long runs taking many hours to be done without requiring the user to respond to the CRRESELE prompts. In this mode, any intermediate files that exist with the given name will automatically be used. If a previous CRRESELE orbit of the same name was interrupted by the user entering "Q" (quit) during execution, and the resulting files still exist, CRRESELE will attempt to pick up where it left off. If an error occurs, then the user should remove the old files or choose a new name for the orbit.

Next, CRRESELE prompts the user for the orbital elements. These elements describe the orbit to be tested. Only orbits for times from day 1, 1985 to day 365, 1999 can be used. There are three options for specifying orbital elements:

Position and Velocity: The elements for position, x, y, z, and velocity, v_x, v_y, v_z, are specified in km and km/sec using the Earth Centered Inertial (ECI) coordinate system. Time is given in year, day of year, hours, minutes, and seconds and must fall between the start of day 1, 1985 and the end of day 365, 1999.

Mean Orbital Elements: Inclination, right ascension of the ascending node, argument of perigee, and mean anomaly are specified in degrees, mean motion is specified in revolutions per day, and eccentricity is specified. Time is given in the same format as for the position and velocity elements.

Solar Elements: Inclination is specified in degrees, while altitudes of apogee and perigee are specified in km (R_E = 6378 km), and local times of apogee and maximum inclination are specified in hours. These elements are useful to scientists and engineers concerned with the location of an orbit with respect to the sun and to those who are not familiar with the standard orbital elements. The solar elements are not a full set of elements because there are only five elements (besides time) to input. The sixth element results from the assumption that the orbit is at apogee at the time for which the elements are specified. Local time of apogee of 12.0 indicates that the satellite is at apogee directly between the sun and Earth. Local time of maximum inclination indicates the local time where the geographic latitude of the satellite is at a maximum positive value. Default values of 12.0 and 18.0 are used respectively for the two local times, but these values may be changed. A 6-hour difference between the local time of apogee and the local time of maximum inclination causes apogee to be at 0° geographic latitude. Oftentimes this arrangement results in the highest fluence since the highest electron concentration is near the magnetic equator, close to the geographic equator. There are other

cases where the 6-hour difference does not result in the highest fluence. One example is an elliptical polar orbit with apogee in the equatorial slot region. The format of the given time is as specified for the position and velocity elements. The solar elements cannot be used by LOKANGL.EXE directly, so CRRESELE converts solar elements into mean orbital elements. (LOKANGL.EXE is described below; see Appendix C for calculations.)

The elements are checked to make sure the orbit is not hyperbolic and perigee is not below 50 km (see Appendix C). The time step used in the study is chosen so that the orbit will sweep $\sim 2°$ arc at perigee in a single time step (see Appendix C). The user then inputs the start time (between day 1 1985 and day 365 1999) and length of the study. The elements are written to an ASCII file called ?NAME?.ELE. After the user is done entering the set of elements, CRRESELE waits for "**D**" to be pressed.

CRRESELE calls LOKANGL.EXE, which reads the element file and generates an ephemeris file, ?NAME?.SPH, which contains geographic position. The position is calculated at each time increment in the specified period of study. Appendix D contains a description of the ?NAME?.SPH file. LOKANGL.EXE is used at the Phillips Laboratory Geophysics Directorate to predict positions of Earth satellites using orbital elements as an input. The code was modified by RADEX Inc. for use on the IBM PC. Contact this office (PL/GPSP) for information on the format of the ?NAME?.ELE file as well as a detailed description of LOKANGL.EXE. LOKANGL.EXE calculates the position of an Earth satellite using a perturbation expansion with the second and third zonal harmonics of Earth's gravitational field. It is not considered accurate for times more than 100 days from a specified orbital element. LOKANGL.EXE cannot evaluate hyperbolic or parabolic orbits or orbits where the radius becomes less that one Earth radius.

CRRESELE calls MAGMODEL.EXE (see Appendix E) to convert the geographic coordinates in ?NAME?.SPH into magnetospheric coordinates that are put into the binary file ?NAME?.MAG, also described in Appendix D. The routines used by MAGMODEL.EXE to calculate L and B/B_0 were developed for the Air Force by Karl Pfitzer at McDonnell Douglas Space Systems Corp (Pfitzer, 1991). The IGRF85 model used by MAGMODEL.EXE is only valid for times after the start of day 1, 1985.

TIMEBINS.EXE is called next by CRRESELE. This program reads the data in the magnetospheric ephemeris file and interpolates between points using a cubic spline to determine how much time the orbit spends in each of the bins defined for the flux models. The resulting array is written to the binary file ?NAME?.TIM.

CRRESELE then calls FLUXDATA.EXE. This program reads in the times in each bin from ?NAME?.TIM and calculates the differential and integral omnidirectional fluence per year as explained

in Section 6, "Fluence Calculations". The integrated data is output to a formatted ASCII file called ?NAME?.DAT. Appendix F shows the contents of SAMPLE.DAT which was generated in Appendix A. The top section gives the name, orbital elements, and the times of the study. After the time of study, the amount of the orbit (by time) not covered by the flux bins is given. An orbit similar to the CRRES orbit is used in SAMPLE.DAT. Since the electron models extend only from L=2.5 to L = 6.55, part of the orbit is out of range of the model. For SAMPLE, this is 12.4 percent (by time), as indicated. The next part of the CRRESELE output is a table showing yearly differential omnidirectional fluences for the 8 models. This is followed by a table showing yearly integral omnidirectional fluences for the 8 models.

At this point CRRESELE has completed its calculations and provides several options to view the data. Pressing "**V**" displays the tables of resulting fluences (file ?NAME?.DAT) on the screen. Pressing "**P**" calls the DOS command "**COPY ?NAME?.DAT PRN**," which will print the ASCII file ?NAME?.DAT. "**D**" graphs the orbit superimposed on the flux models using ELECDISP.EXE (see Appendix E), and "**G**" graphs the orbit using ORBIT.EXE (described in Appendix E). "**Q**" quits CRRESELE. A benchmark file is created by CRRESELE showing how long each of the different utilities took to run. This file has the name ?NAME?.BEN and is discussed in more detail in Appendix A.

References

Brautigam, D.H., Gussenhoven, M.S., and Mullen, E.G. (1992) Quasi-static model of outer zone electrons. *IEEE Trans. Nucl. Sci.* **39**:1797.

McIlwain, C.E. (1961) Coordinates for mapping the distribution of magnetically trapped particles, *J. Geophys. Res.*, **66**:3681.

IAGA Division I, Working Group 1. (1986) International geomagnetic reference field revision 1985. *EOS, Trans., Am. Geophys. U.* **67** (No. 24).

Knecht, D.J., and Shuman, B.M. (1985) "The Geomagnetic Field", Chapter 4 in *Handbook of Geophysics and the Space Environment*, edited by Adolph S. Jursa. Air Force Geophysics Laboratory, Hanscom AFB, MA. ADA167000.

Olson, W.P., and Pfitzer, K.A. (1974) A quantitative model of the magnetospheric magnetic field. *J. Geophys. Res.*. **79**:3739.

Spjeldvik, W.N., and Rothwell, P.L. (1985) "The Radiation Belts", Chapter 5 in *Handbook of Geophysics and the Space Environment*, edited by Adolph S. Jursa. Air Force Geophysics Laboratory, Hanscom AFB, MA. ADA167000.

NOAA-USAF Space Environment Services Center, *Preliminary Report and Forecast of Solar Geophysical Data*, U.S. Dept. of Commerce, NOAA, Boulder, CO.

NOAA World Data Center-A, *Solar Geophysical Data prompt reports*, U.S. Dept. of Commerce, NOAA E/GC2, Boulder, CO.

NOAA-USAF Space Environment Services Center. (1988) *SESC Glossary of Solar-Terrestrial Terms*, U.S. Dept. of Commerce, NOAA, Boulder, CO.

Hunerwadel, J.L., Sellers, B., and Hanser, F.A. (1987), *Design, Fabricate, Calibrate, and Deliver Two Satellite Electron Flux Detectors*, AFGL-TR-87-0205, Air Force Geophysics Laboratory, Hanscom AFB, MA, ADA190799.

Dichter, B.K., and Hanser, F.A. (1989), *Development and Use of Data Analysis Procedures for the CRRES Payloads AFGL-701-2/Dosimeter and AFGL-701-4/Fluxmeter and Application of the Data Analysis Results to Improve the Static and Dynamic Models of the Earth's Radiation Belts*, GL-TR-89-0284, Contract F19628-87-C-0169, Panametrics, Inc., ADA219479.

Dichter, B.K., and Hanser, F.A. (1991), *Development and Use of Data Analysis Procedures for the CRRES Payloads AFGL-701-2/Dosimeter and AFGL-701-4/Fluxmeter and Application of the Data Analysis Results to Improve the Static and Dynamic Models of the Earth's Radiation Belts*, PL-TR-91-2186, Contract F19628-87-C-0169, Panametrics, Inc., ADA241399.

Dichter, B.K., and Hanser, F.A. (1992), *Development and Use of Data Analysis Procedures for the CRRES Payloads AFGL-701-2/Dosimeter and AFGL-701-4/Fluxmeter and Application of the Data Analysis Results to Improve the Static and Dynamic Models of the Earth's Radiation Belts*, PL-TR-92-2223, Contract F19628-87-C-0169, Panametrics, Inc., ADA258710.

Hanser, F.A. (1995,to be published), *Analyze Data from CRRES Payloads AFGL-701-2/Dosimeter and AFGL-701-4/Fluxmeter*, PL-TR-95-2103, Contract F19628-92-C-0020, Panametrics, Inc.

Blake, J.B., Kolasinski, W.A., Filius, R.W., and Mullen, E.G. (1992) Injection of electrons and protons with energies of tens of MeV into $L<3$ on March 24, 1991. *Geophys. Res. Lett.*, Vol. 19, 821.

Mullen, E.G., Gussenhoven, M.S., Ray, K., and Violet, M. (1991) A double-peaked inner radiation belt: cause and effect as seen on CRRES. *IEEE Trans. Nucl. Sci.*, **38**: 1713.

Pfitzer, K.A. (1991) *Improved Models of the Inner and Outer Radiation Belts*. PL-TR-91-2187, Contract F19628-90-C-0099, McDonnell Douglas Space Systems Corp., ADA242579.

U.S. Naval Observatory. (1992) *The Astronomical Almanac for the Year 1992*. Nautical Almanac office, United States Naval Observatory, Washington, D.C., p B6.

Gussenhoven, M.S., Mullen, E.G., and Brautigam, D.H. (to be published, April,1996) Improved Understanding of the Earth's Radiation Belts from the CRRES Satelllite. *IEEE Trans. Nucl. Sci.* (special issue).

Mullen, E.G. and Holeman, E. (1994) MeV Electrons as Measured by the DMSP J4 Detector part 1: Particle Identification and Verification. *EOS, Trans. Am. Geophys. U.*, Vol. 75, November 1 Supplement, p 541.

Appendix A

Sample Session

Type:

CRRESELE <Enter>

Press any key once you have read the information on the screen. You are now asked for a file name. Here we use "SAMPLE" as the file name. Type:

SAMPLE <Enter>

Press any key once you have read the information on the screen. Press "**S**" to select solar elements. On the next screen we specify an orbit that is very similar to the orbits used by CRRES. Enter the solar elements and the time for which those elements apply:

Year = **1991**
Day = **130**
Hour = **8**
Minute = **0**
Second = **0**
Inclination = **18**
Alt Perigee = **350**
Alt Apogee = **33000**

Leave the two default local times as they are at **12** and **18**. This causes the satellite to be at apogee at 12:00 and at maximum inclination at 18:00 local time. (See Section 3 for the applicable logic.) If you enter something incorrectly, you can tab back to that line and enter it again. Pressing "**x**" then <Enter> on a line will delete it. When you are done press "**D**." At the next screen enter the time of the study:

Year = **1991**
Day = **130**
Hour = **8**
Minute = **0**
Second = **0**
Length = **1** (days)

The time of the study can differ from the time entered previously for the element information. Press "**D**" when you are done. The modules LOKANGL, MAGMODEL, TIMEBINS, and FLUXDATA will now execute sequentially. Upon completion, a screen will appear explaining various options for proceeding. On hitting any key, you will be presented with a menu that allows you to select these options. If you have a printer, press "**P**" to get a printout. (Appendix F is a copy of the printout of the file SAMPLE.DAT.) You can press "**V**" to see the output on the screen. "**Q**" will return you to the menu. Pressing "**G**" calls ORBIT.EXE to show the orbit plot. The view in the lower right looks down on Earth's north pole with the sun towards the top. The other two images show side views, looking along X and Y. The orientation of the axes on these views follows standard drafting conventions. "**D**" executes ELECDISP.EXE which shows the orbit track through the radiation belts. The orbit track is plotted entirely in the upper quadrant because when the orbit coordinates are converted from geographic to magnetic coordinates (L, B/B_0), latitudinal information is lost.

The actual CPU time required to complete an individual run (create fluence ASCII file) will vary with the speed of the computer, the type of orbit, and the length of study. In general, lower altitudes take longer than higher altitudes, elliptical orbits take longer than circular, high inclination orbits take longer than low inclination, and, obviously, the runtime increases with the length of the study. It is recommended that if CRRESELE is to be run for a time interval length on the order of months, a few initial runs for time lengths on the order of a day first be made so as to estimate the runtime required. To facilitate the estimate of the runtime, a 'benchmark' file (filename.ben) is created for each individual run. The CPU runtime for orbit "SAMPLE" is recorded in the ASCII benchmark file called SAMPLE.BEN. The following is a copy of the bench mark file for SAMPLE when run on a 66 MHz 486 GATEWAY computer at Phillips Laboratory:

*****

Time increment = 136.64 seconds.

15:53:14.41 --> LOKANGL started

15:53:17.21 --> LOKANGL finished

Number of points = 635

15:53:18.80 --> MAGMODEL started

15:53:28.25 --> MAGMODEL finished

15:53:29.89 --> TIMEBINS started

15:53:30.11 --> TIMEBINS finished

15:53:31.71 --> FLUXDATA started

15:53:31.98 --> FLUXDATA finished

Time increment (136.64 s) is the step size chosen by CRRESELE to calculate ephemeris and fluence. This time was chosen so that the satellite swings through approximately 2° arc at perigee. See Appendix C for calculations. The orbit trace was divided into 635 spatial bins ($L,B/B_0$). LOKANGL took 2.8 seconds to run, MAGMODEL took 9.45 seconds, TIMEBINS took 0.22 second, and FLUXDATA took 0.27 second. The total CPU time was 12.74 seconds. For this particular orbit, the time required for LOKANGL and MAGMODEL to run is directly proportional to the time 'length' of study. The runtime for FLUXDATA depends only on the orbit and not on the 'length' of study. TIMEBINS requires the least amount of CPU time to execute.

Appendix B

Format of FLUX_MOD.## Files

The FLUX_MOD.## files contain data binned by L and B/B_0. Any rate data such as flux or dose rate can be put into these files, provided the following format is used:

- The filename must be FLUX_MOD.## (## = 00 to 79)

- The file structure is of the type:

-- BORLAND PASCAL

```
Type
 FluxRecord = record
     MainTitle,
     SubTitle,
     Units      :  String[136];
     d          :  Array[1..81,1..34] of Single;
 end;
```

-- ANY OTHER LANGUAGE

MainTitle,

SubTitle,

Units : Each is an array of 136 eight bit bytes or characters. The first byte

contains the number of characters in the array (0 to 136). The following bytes contain the characters in the array.

d : This is the data. Each bin is a 4 byte real number following the convention set by the Intel math coprocessor. The data is binned in a two dimensional array of 1 to 81 (L) by 1 to 34 (B/B_0). Consecutive B/B_0 bins occupy consecutive spaces in memory.

- The files have four different groups of information.

-- The first three groups are strings. **MainTitle** and **SubTitle** are strings of characters that are displayed as the two title lines by the utility ELECDISP.EXE. **Units** is the string displayed by ELECDISP.EXE near the scale to identify what type of data is displayed.

-- The fourth group is the data. **d** is a two dimensional array of 1 to 81 (L) by 1 to 34 (B/B_0) bins.

--- **i** is the index associated with L, and ranges from 1 to 81. The limits of bins with index **i** are: $2.45+0.05\mathbf{i}\ R_E \leq L < 2.50+0.05\mathbf{i}\ R_E$

--- **j** is the index associated with B/B_0, and ranges from 1 to 34. The limits of bins with index **j** are:

$B_{j-1} \leq B/B_0 < B_j$;

$B_{0...34}$ = 1.000, 1.004, 1.020, 1.046, 1.085, 1.140, 1.200, 1.300, 1.400, 1.520, 1.690, 1.880, 2.100, 2.400, 2.730, 3.130, 3.670, 4.350, 5.020, 6.100, 7.410, 9.088, 1.129e1, 1.422e1, 1.816e1, 2.356e1, 3.107e1, 4.147e1, 5.723e1, 8.025e1, 1.154e2, 1.707e2, 2.607e2, 4.134e2, 6.846e2. (where e# indicates $(\cdot 10^{\#})$.)

--- The values of B_j are such that the limits B_0 to B_{34} cover approximately $\pm 68°$ magnetic latitude in a dipole field.

Appendix C

Calculations Used to Create Element File

We give here the equations used to 1) calculate the time step used in LOKANGL.EXE, 2) convert solar elements to mean orbital elements, and 3) eliminate invalid orbits, namely those that are not closed or that pass close to or beneath the surface of Earth. Two constants specific to Earth that are used throughout are μ, the gravitational constant times the mass of Earth, and R_E, the radius of Earth assuming Earth is spherical. These values are:

$\mu = 398601.2 \text{ km}^3\text{sec}^{-2}$,
$R_E = 6378.145$ km.

(1) Time Step Calculation:

If Position/Velocity Elements are used where

$$r = \sqrt{r_x^2 + r_y^2 + r_z^2} \quad , \quad v = \sqrt{v_x^2 + v_y^2 + v_z^2} \ ,$$

then define the three quantities, a, h, and e as

$$a^{-1} = \frac{2}{r} - \frac{v^2}{\mu} \quad , \quad h = |\vec{r} \times \vec{v}| \quad , \quad e^2 = 1 - \frac{h^2}{\mu a} \quad .$$

Here a is the semimajor axis in km, h is the angular momentum in km^2/sec, and e is the eccentricity.

If Mean Orbital Elements are used, the eccentricity e and the mean motion M_m in revolutions per day are given as elements. The semimajor axis a and the magnitude of the angular momentum h are

given by:

$$a^3 = \mu[(12 \cdot 3600)/(\pi M_m)]^2 \quad , \quad h^2 = \mu a(1-e^2) \quad .$$

In terms of a, h, and e, the time step T_s, which is approximately equal to the time to traverse 2° arc at perigee is:

$$T_s = a^2(1-e^2)h^{-1}\frac{\pi}{90} \quad .$$

In this calculation $d\Theta/dt$ at perigee is assumed to be constant over the 2° arc.

(2) To Convert Solar Elements to Mean Elements:

Use the convention: day = 1 on 1 January 1992.

Define the following quantities:

$r_a = A_a + R_E$;

$r_p = A_p + R_E$; A_a and A_p are altitudes from the surface of Earth in km;

$H_e = 6.594703 + 0.0657098243 \cdot day + 1.00273791 \cdot Hr$ (U.S. Naval Observatory, 1992);

$\Theta_a = (H_a + 12)*\pi/12$, where H_a is local time of apogee;

$\Theta_i = (H_i - 6)*\pi/12$, where H_i is local time of maximum inclination.

Then the six elements are:

inclination, i, is given;

eccentricity, $e = (r_a - r_p) / (r_a + r_p)$;

mean anomaly, M = 180° (satellite is at apogee when elements are defined);

squared mean motion, $n^2 = \mu/[\frac{1}{2}(r_a+r_p)]^3(12 \cdot 3600/\pi)^2$;

right angle of ascending node, $\Omega = 15(H_i - 6 + H_e)$;

argument of perigee, ω, $\cos(\omega) = \cos(\Theta_a)\cos(\Theta_i) + \sin(\Theta_a)\sin(\Theta_i)$.

(3) Check Elements for valid orbit:

The orbit is valid if:

a) the orbit is closed: $0 \leq e^2 < 1$;

b) perigee is not below the surface of Earth: $a(1-e) \geq 6400$ km.

Appendix D

Format of Ephemeris Files

The geographic ephemeris files end with the extension "SPH." These are binary files that are output from LOKANGL.EXE. Each record of the file specifies the position of a satellite, and the time interval between all records is constant (T_s is in Appendix C). These files are input by MAGMODEL.EXE to produce the magnetospheric ephemerides.

Each record of the file contains, in the following order:

year	: 2 byte integer
day	: 2 byte integer
second	: 4 byte real
latitude	: 4 byte real (deg)
longitude	: 4 byte real (deg)
radius	: 4 byte real (km)

The magnetospheric ephemeris files end with the extension "MAG." These are binary files that are output from MAGMODEL.EXE. Each record of the file specifies the position of a satellite in Earth's magnetic field, and the time interval between the records is constant (T_s). The requirement for a constant time step is set by TIMEBINS.EXE. These files are input by TIMEBINS.EXE to produce files indicating how much time the orbit spends in the magnetospheric bins defined for the flux models (see Appendix B).

Each record of a ".MAG" file contains, in the following order:

L	: 4 byte real
B/B_0	: 4 byte real

Open field lines are indicated by an L of -1 or $L > 15\ R_E$.

The last record of each file contains, in the following order:

-100	: 4 byte real
TimeStep	: 4 byte real (time interval between steps)

LOKANGL.EXE can be bypassed by creating a ".SPH" ephemeris file of the proper format. CRRESELE will still request orbital elements so you must generate a dummy element file, but CRRESELE will not execute LOKANGL.EXE if the ".SPH" file exists. In the same way, a different magnetospheric model can be used by creating a ".MAG" file of the proper format. CRRESELE will still request orbital elements, and will run LOKANGL.EXE (if a ".SPH" file does not exist), but it will not execute MAGMODEL.EXE.

Appendix E

CRRESELE Support Programs

ORBIT.EXE - This is a display utility program that works on a color EGA/VGA monitor. It is

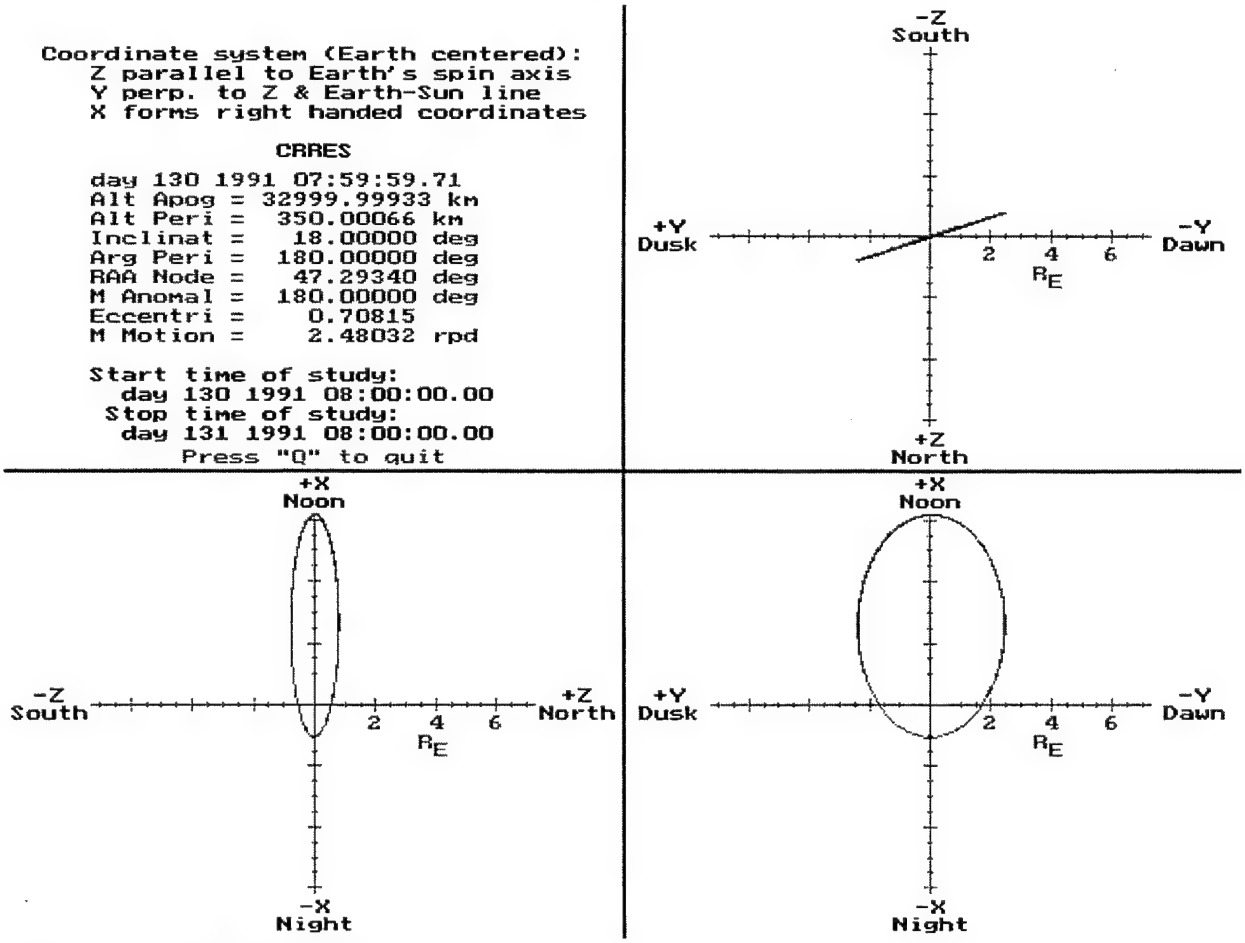

Figure E1. ORBIT.EXE Screen.

called by CRRESELE, but may also be called from the command line. This program reads the ".SPH" files, and will also read the ".DAT" files if they exist. When calling ORBIT.EXE from the command line, the name of the run must be included on the command line. The name of these files may include a path, but not an extension. If one typed "**ORBIT \ORB\SAMPLE**," the data file SAMPLE.SPH in the directory "\ORB" would be displayed. If SAMPLE.DAT exists then orbital elements read from that file would be displayed in the upper left corner. Figure E1 shows a screen capture of ORBIT.EXE using the files created in the sample session of Appendix A. The upper left corner shows information about the orbit drawn. The lower right-hand corner shows the orbit projected into the XY plane. Tick marks show integral values of R_E. The other two corners show the orbit projected into the XZ and YZ planes. The orientation of the coordinates follows drafting convention where the figure in the lower right corner is the top view and the other two figures are side views. In the coordinate system used (see Figure E2), **Z** points along Earth's spin axis and is positive toward the north pole, while **Y** is perpendicular to **Z** and the Earth-Sun line and is positive towards dusk. **X** completes the right handed coordinate system and goes through the noon meridian. Pressing "**Q**" exits this display program.

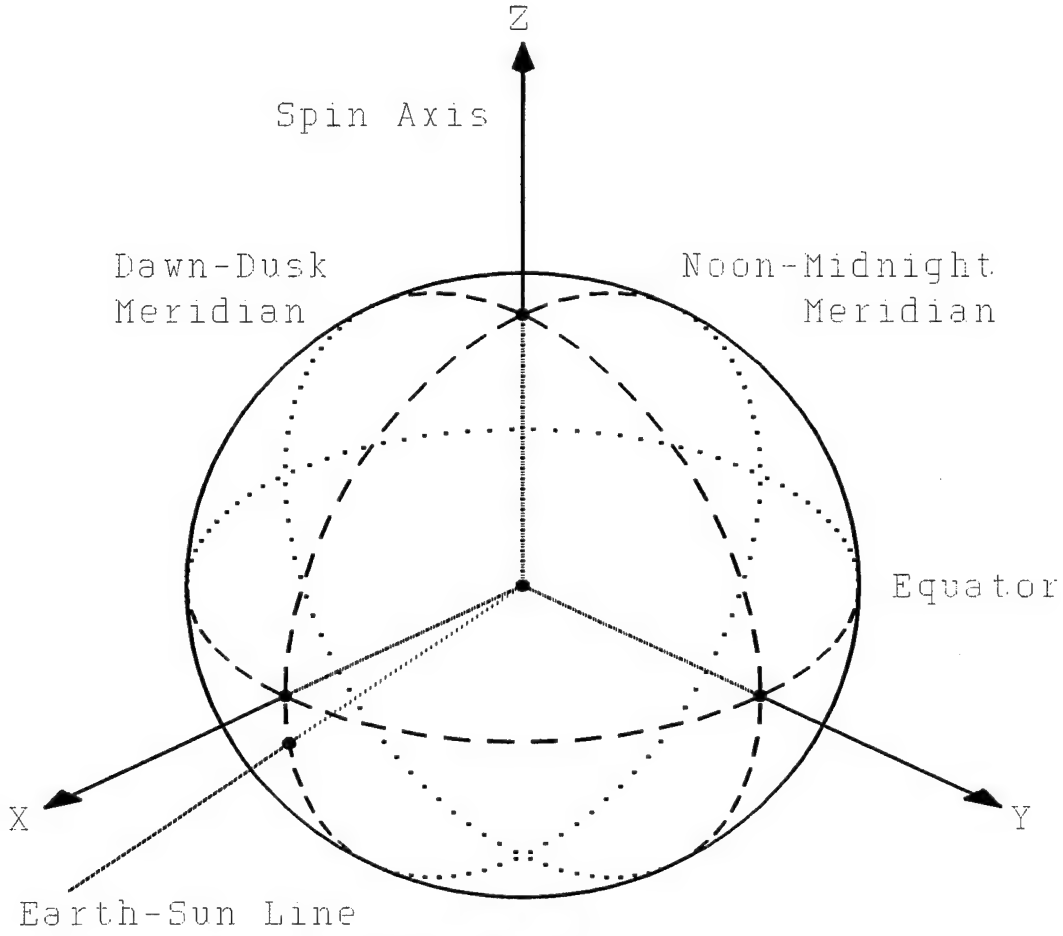

Figure E2. Coordinate System Used for ORBIT.EXE.

MAGMODEL.EXE - This program uses the IGRF85 and Olson-Pfitzer Static Magnetic Field Model IBM PC Fortran routines developed by Karl Pfitzer (1991). To use this code two command line parameters are required. The first is the path of the source file (including name and extension), and the second is the path of the destination file (including name and extension). The source file is a geographic ephemeris file, and the destination file is a magnetospheric ephemeris file. The formats of both these files are described in Appendix D.

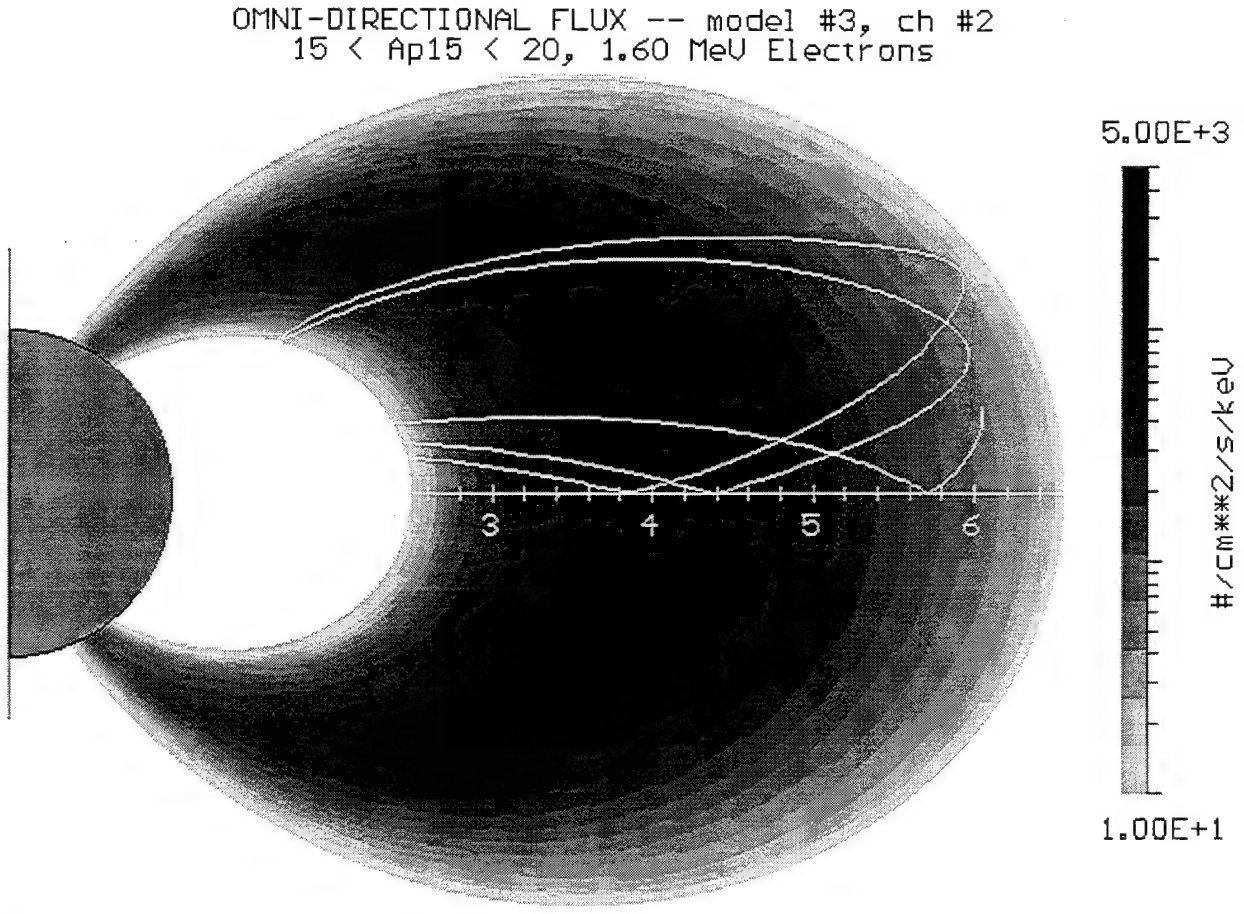

File 32
Figure E3. ELECDISP.EXE Screen Displaying SAMPLE.MAG Orbit.

ELECDISP.EXE - This program displays the flux data in the FLUX_MOD.## files. The data is placed spatially on the screen as it would look if Earth's magnetic field were a dipole. (The image will not be proportioned correctly if an EGA card is used). Figure E3 shows a copy of the screen when ELECDISP.EXE is displaying the orbit generated in Appendix A. Although the figure here is in gray scale, the CRRESELE screen display is in color. The following description explains what is seen here (in gray scale). The half circle on the left side of the screen represents Earth with the magnetic axis

pointing straight up. Gray scales represent intensity of flux. Higher flux tends toward the darker shading, and lower flux tends toward the lighter shading. If the flux is above the color scale, it will be shown as black, and if the flux is below the color scale or there is no data, it will be shown as light gray. The display on the computer screen will show Earth as a cyan colored half circle. Color scales represent the intensity of flux. Higher flux tends toward red and lower flux tends toward blue. Flux above the color scale is shown in white, and flux below the color scale is shown in gray. The space bar calls up an options menu. The color scale can be reset and can also be changed from a log to a linear scale. One can move to a higher (lower) flux model by pressing the plus (minus) key. Pressing "**Q**" quits the program. The orbit in L versus B/B_0 is plotted as a black line on the upper quadrant of the flux data. The orbit is plotted in only one quadrant because B/B_0 contains no information about +/- latitude. This causes the orbit to be folded into the upper quadrant. In Figure E3, the orbit covers the area from Earth's surface to below the L cutoff of 6.55. The flux model in Figure E3 shows omnidirectional flux for 1.60 MeV electrons during a moderately active time period ($15 < Ap_{15} < 20$). The outer zone electron belt peaks around $L=4.2\ R_E$.

The orbit plot superimposed on the flux data can be used to analyze the effectiveness of CRRESELE for the given orbit. Portions of low orbits may actually be drawn below Earth's surface on the plots. This results from the fact that Earth is not actually spherical, the magnetic field is not actually dipolar, and the center of the magnetic field is not at the center of Earth.

ELECDISP.EXE can be run from the command line by typing "**ELECDISP**." ELECDISP will ask for the file number to be displayed, and will then graph the data. The file number can also be specified on the command line. To show FLUX_MOD.09 one would type "**ELECDISP 9**." A second command line parameter can be included to show an orbit superimposed on the flux map. The second parameter must be the path (including name and extension) of a magnetospheric ephemeris file. The file must be in the format given in Appendix D.

Appendix F

Contents of SAMPLE.DAT

CRRESELE Prediction Utility - CRRES

Element time: day 130 1991 07:59:59.71

Alt Apog = 33000.00 km	Alt Peri = 350.00 km
Inclinat = 18.00 deg	Arg Peri = 180.00 deg
RAA Node = 47.29 deg	M Anomal = 180.00 deg
Eccentri = 0.708	M Motion = 2.48 rpd

Start time of study: day 130 1991 08:00:00.00

Stop time of study: day 131 1991 08:00:00.00

Time of study is 1.000 days (12.4 % of orbit out of range)

Omnidirectional fluence/year [#/(cm^2 keV year)]:

Model Number	Ave Energy	Fluence
0	0.65 MeV	5.82E+0010
0	0.95 MeV	1.55E+0010
0	1.60 MeV	6.49E+0008
0	2.00 MeV	8.03E+0007
0	2.35 MeV	1.78E+0007
0	2.75 MeV	3.93E+0006
0	3.15 MeV	1.10E+0006

Omnidirectional fluence/year [#/(cm^2 keV year)]:

Model Number	Ave Energy	Fluence
0	3.75 MeV	1.97E+0005
0	4.55 MeV	4.26E+0004
0	5.75 MeV	1.18E+0004
1	0.65 MeV	1.14E+0011
1	0.95 MeV	3.63E+0010
1	1.60 MeV	1.64E+0009
1	2.00 MeV	2.41E+0008
1	2.35 MeV	6.57E+0007
1	2.75 MeV	2.11E+0007
1	3.15 MeV	7.29E+0006
1	3.75 MeV	1.61E+0006
1	4.55 MeV	2.18E+0005
1	5.75 MeV	4.75E+0004
2	0.65 MeV	2.06E+0011
2	0.95 MeV	7.57E+0010
2	1.60 MeV	5.89E+0009
2	2.00 MeV	1.07E+0009
2	2.35 MeV	3.19E+0008
2	2.75 MeV	1.07E+0008
2	3.15 MeV	3.99E+0007
2	3.75 MeV	9.28E+0006
2	4.55 MeV	1.23E+0006
2	5.75 MeV	2.85E+0005
3	0.65 MeV	2.39E+0011
3	0.95 MeV	1.04E+0011
3	1.60 MeV	1.05E+0010
3	2.00 MeV	1.95E+0009
3	2.35 MeV	5.71E+0008

Omnidirectional fluence/year [#/(cm^2 keV year)]:

Model Number	Ave Energy	Fluence
3	2.75 MeV	1.86E+0008
3	3.15 MeV	6.95E+0007
3	3.75 MeV	1.69E+0007
3	4.55 MeV	2.37E+0006
3	5.75 MeV	4.44E+0005
4	0.65 MeV	3.51E+0011
4	0.95 MeV	1.74E+0011
4	1.60 MeV	1.75E+0010
4	2.00 MeV	3.32E+0009
4	2.35 MeV	9.59E+0008
4	2.75 MeV	3.06E+0008
4	3.15 MeV	1.19E+0008
4	3.75 MeV	3.12E+0007
4	4.55 MeV	4.70E+0006
4	5.75 MeV	9.29E+0005
5	0.65 MeV	4.75E+0011
5	0.95 MeV	2.81E+0011
5	1.60 MeV	3.34E+0010
5	2.00 MeV	6.41E+0009
5	2.35 MeV	1.63E+0009
5	2.75 MeV	4.46E+0008
5	3.15 MeV	1.67E+0008
5	3.75 MeV	4.13E+0007
5	4.55 MeV	6.54E+0006
5	5.75 MeV	1.58E+0006
6	0.65 MeV	2.77E+0011
6	0.95 MeV	1.36E+0011
6	1.60 MeV	1.42E+0010

Omnidirectional fluence/year [#/(cm^2 keV year)]:

Model Number	Ave Energy	Fluence
6	2.00 MeV	2.68E+0009
6	2.35 MeV	7.22E+0008
6	2.75 MeV	2.16E+0008
6	3.15 MeV	8.13E+0007
6	3.75 MeV	2.02E+0007
6	4.55 MeV	3.11E+0006
6	5.75 MeV	6.78E+0005
7	0.65 MeV	1.29E+0012
7	0.95 MeV	1.18E+0012
7	1.60 MeV	2.61E+0011
7	2.00 MeV	5.87E+0010
7	2.35 MeV	1.64E+0010
7	2.75 MeV	4.68E+0009
7	3.15 MeV	1.86E+0009
7	3.75 MeV	5.05E+0008
7	4.55 MeV	1.13E+0008
7	5.75 MeV	3.45E+0007

Integral Omnidirectional Fluence/year [#/(cm^2 year)] to 6.60 MeV:

Model Number	Ave Energy	Fluence
0	0.50 MeV	2.48E+0013
0	0.85 MeV	5.63E+0012
0	1.25 MeV	3.33E+0011
0	1.70 MeV	4.15E+0010
0	2.10 MeV	9.33E+0009
0	2.50 MeV	2.22E+0009
0	2.90 MeV	6.54E+0008
0	3.30 MeV	2.13E+0008

Integral Omnidirectional Fluence/year [#/(cm^2 year)] to 6.60 MeV:

Model Number	Ave Energy	Fluence
0	4.10 MeV	5.57E+0007
0	4.95 MeV	1.95E+0007
1	0.50 MeV	5.10E+0013
1	0.85 MeV	1.33E+0013
1	1.25 MeV	8.74E+0011
1	1.70 MeV	1.36E+0011
1	2.10 MeV	3.92E+0010
1	2.50 MeV	1.29E+0010
1	2.90 MeV	4.47E+0009
1	3.30 MeV	1.55E+0009
1	4.10 MeV	2.63E+0008
1	4.95 MeV	7.83E+0007
2	0.50 MeV	9.76E+0013
2	0.85 MeV	2.93E+0013
2	1.25 MeV	3.27E+0012
2	1.70 MeV	6.22E+0011
2	2.10 MeV	1.95E+0011
2	2.50 MeV	6.76E+0010
2	2.90 MeV	2.49E+0010
2	3.30 MeV	8.94E+0009
2	4.10 MeV	1.52E+0009
2	4.95 MeV	4.70E+0008
3	0.50 MeV	1.21E+0014
3	0.85 MeV	4.17E+0013
3	1.25 MeV	5.86E+0012
3	1.70 MeV	1.13E+0012
3	2.10 MeV	3.47E+0011
3	2.50 MeV	1.19E+0011

Integral Omnidirectional Fluence/year [#/(cm^2 year)] to 6.60 MeV:

Model Number	Ave Energy	Fluence
3	2.90 MeV	4.41E+0010
3	3.30 MeV	1.63E+0010
3	4.10 MeV	2.75E+0009
3	4.95 MeV	7.32E+0008
4	0.50 MeV	1.88E+0014
4	0.85 MeV	6.98E+0013
4	1.25 MeV	9.80E+0012
4	1.70 MeV	1.91E+0012
4	2.10 MeV	5.84E+0011
4	2.50 MeV	2.01E+0011
4	2.90 MeV	7.82E+0010
4	3.30 MeV	3.04E+0010
4	4.10 MeV	5.52E+0009
4	4.95 MeV	1.53E+0009
5	0.50 MeV	2.76E+0014
5	0.85 MeV	1.16E+0014
5	1.25 MeV	1.85E+0013
5	1.70 MeV	3.50E+0012
5	2.10 MeV	9.37E+0011
5	2.50 MeV	2.86E+0011
5	2.90 MeV	1.08E+0011
5	3.30 MeV	4.12E+0010
5	4.10 MeV	8.17E+0009
5	4.95 MeV	2.61E+0009
6	0.50 MeV	1.48E+0014
6	0.85 MeV	5.48E+0013
6	1.25 MeV	7.88E+0012
6	1.70 MeV	1.50E+0012

Integral Omnidirectional Fluence/year [#/(cm^2 year)] to 6.60 MeV:

Model Number	Ave Energy	Fluence
6	2.10 MeV	4.27E+0011
6	2.50 MeV	1.39E+0011
6	2.90 MeV	5.24E+0010
6	3.30 MeV	1.99E+0010
6	4.10 MeV	3.76E+0009
6	4.95 MeV	1.12E+0009
7	0.50 MeV	1.01E+0015
7	0.85 MeV	5.67E+0014
7	1.25 MeV	1.51E+0014
7	1.70 MeV	3.32E+0013
7	2.10 MeV	9.74E+0012
7	2.50 MeV	3.17E+0012
7	2.90 MeV	1.30E+0012
7	3.30 MeV	5.57E+0011
7	4.10 MeV	1.53E+0011
7	4.95 MeV	5.70E+0010

Appendix G

Outline of Data Processing Procedures

This appendix outlines the complete data processing procedure followed, beginning with the unprocessed data files, to obtain the final smoothed equatorial pitch angle distributions for a given model. These pitch angle distributions are then projected down the magnetic field line to the 34 different B/B_0 values (for each of 81 L bins), where they are then integrated over pitch angle to determine the omnidirectional fluxes used in fluence calculations.

1. Begin with original CRRES Time History Database orbit files for the HEEF instrument (*D04nnnn*, nnnn=orbit number 0001-1067) containing packed data for each 0.512 second observation period.

2. Create a new set of orbit files, *D04nnnn.LXD*, from *D04nnnn* as follows:
   a. Unpack data and correct for "roll-overs" in the front solid state detetector counters.
   b. Bin data into eighty-one 0.05 Re L bins (L=2.5-6.55) and nineteen 5° pitch angle bins (α=0°-90°); Accumulate total counts and total number of observations (obs).
   c. Determine average counts per second by dividing total counts by (obs·0.512 secs).

3. Create new set of files, *D04nnnn.FLX*, from *D04nnnn.LXD* as follows:
   a. Perform full set of corrections for deadtime, temperature, and "paralyzation" effects as discussed in (Dichter and Hanser, 1992; Hanser, 1995). Convert counts/sec to flux.

4. Create single database file consisting of daily average equatorial fluxes, *EQFLX1.DAT*, from *D04nnnn.LXD* by following steps 4a-4d for each single day of data (1 day = approximately 2.4 orbits):
   a. Examine the pitch angle distribution (PAD: flux vs pitch angle at constant energy) for each L

bin. When there are data in at least 9 out of 19 pitch angle bins for a given PAD, fit the PAD to a $\sin^n\alpha$ curve. If the correlation coefficient of the fit is at least 0.75, replace the data with the fitted points. A sample pitch angle distribution (PAD) from orbit 939 illustrating this procedure is shown in Figure G1 below. This particular case corresponds to the L=5.00-5.05 bin, with $B/B_0=1.27$ (magnetic latitude= -11.9 degrees). The open squares designate the L bin averaged PAD, and include pitch angle data from 90° down to 15°. The curve marked by the '+' symbol is the $\sin^n\alpha$ fit to the L bin averaged PAD (n=1.54 , correlation coefficient=0.93). The fitted PAD has filled in the data gaps at the lowest pitch angles down to 0°.

b. Each PAD, fitted or otherwise, is mapped to the equator. In the sample PAD shown in Figure G2, the final equatorial PAD is designated by the curve with filled triangles (n=1.65). Mapping a PAD to the magnetic equator, from a point off the magnetic equator, results in a flux deficit at equatorial pitch angles near 90° because these particles mirror near the equator and are not detected at points that are increasingly distant from the equator. However, if the original PAD is successfully

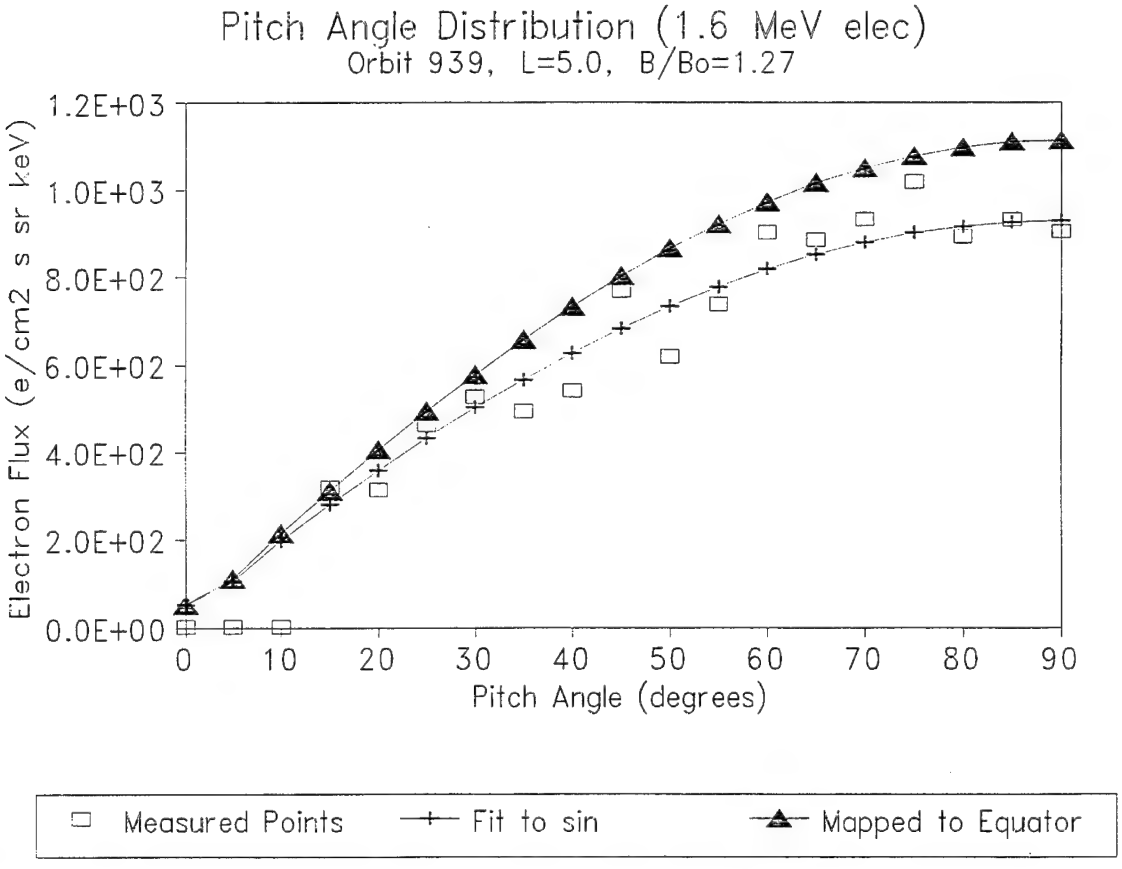

Figure G1. Pitch angle distribution is first fit to $\sin^n\alpha$ and then mapped back to the equator.

fit to a $\sin^n\alpha$ curve, then the equatorial PAD will be as well, and this enables one to fill any missing pitch angle bin data. These equatorial PADs are binned into daily averages.

5. Daily averages are separated into 8 models (6 CRRES_Ap models, 1 CRRES_AVE model, 1 CRRES_MAX model) as explained in Section 4.

6. A large degree of scatter due to low count rates and/or missing data is observed in many of the equatorial pitch angle distributions, particularly at the higher energies. Data are often missing at the endpoints of the PADs (that is, at 0-20° and/or 80-90°) because of the satellite's orientation to the magnetic field or because of the effect of mapping the PAD back to the equator. The following technique is employed to smooth the data.

a. Individually fit all the model equatorial pitch angle distributions to a $\sin^n\alpha$ curve. Save the sine index **n** for all PADs for which there were at least 9 points and which yielded a correlation coefficient of at least 0.75. Perform a linear regression on **n** as a function of energy, independent of L and model. This regression yields the relation: $\mathbf{n(E) = 0.23 \cdot E + 0.35}$ (where E is energy in MeV) with a correlation coefficient of 0.89.

b. Determine the omnidirectional flux L profile for a given energy and model, and smooth this curve using the commercial software package *TableCurve* (Jandel Scientific). This smoothed omni-directional flux profile may then, assuming a $\sin^n\alpha$ PAD, be transformed back to a directional flux profile (as a function of pitch angle) as shown in the next step.

c. The omnidirectional flux, J_{omni}, is related to the directional flux, $j(\alpha)$, as follows:

$$J_{omni} = 4\pi \int_{0^\circ}^{90^\circ} j(\alpha)\sin(\alpha)d\alpha$$

The directional flux has been shown, in most instances, to be well modeled by $j(\alpha) = j_{90} \sin^n\alpha$, where j_{90} is the flux at $\alpha=90°$. The omnidirectional flux may then be written as:

$$J_{omni} = 4\pi \int_{0^\circ}^{90^\circ} j_{90}\sin^{n+1}(\alpha)d\alpha$$

Solving for j_{90}, we find:

$$j_{90} = \frac{J_{omni}(n)}{I(n)}, \qquad where \qquad I(n) = 4\pi \int_{0^\circ}^{90^\circ} \sin^{n+1}(\alpha) d\alpha$$

The integral (I) is numerically performed for a number of discrete values of n spanning the range of observed values. The resulting curve, I(n), is analytically fit by *TableCurve*, and is expressed as:

$$I(n) = 4\pi \sqrt{\frac{1.3189}{\sqrt{n+1}} - 0.3155}$$

This permits the transformation from the smoothed equatorial omnidirectional fluxes to the desired smoothed equatorial directional fluxes as $j(\alpha) = J_{omni}\sin^n\alpha$ / I, where n=n(E) is given in step 6a.

Figure G2 illustrates the effect of the smoothing procedure described above. The left (right) hand panel presents plots of the unsmoothed (smoothed) fluxes for all 8 models at 3.75 MeV. The bottom two curves in each panel are the flux profiles for the two lowest activity models, and involve the most scatter. The effect of smoothing is neglible on the higher activity models where there are higher counter rates.

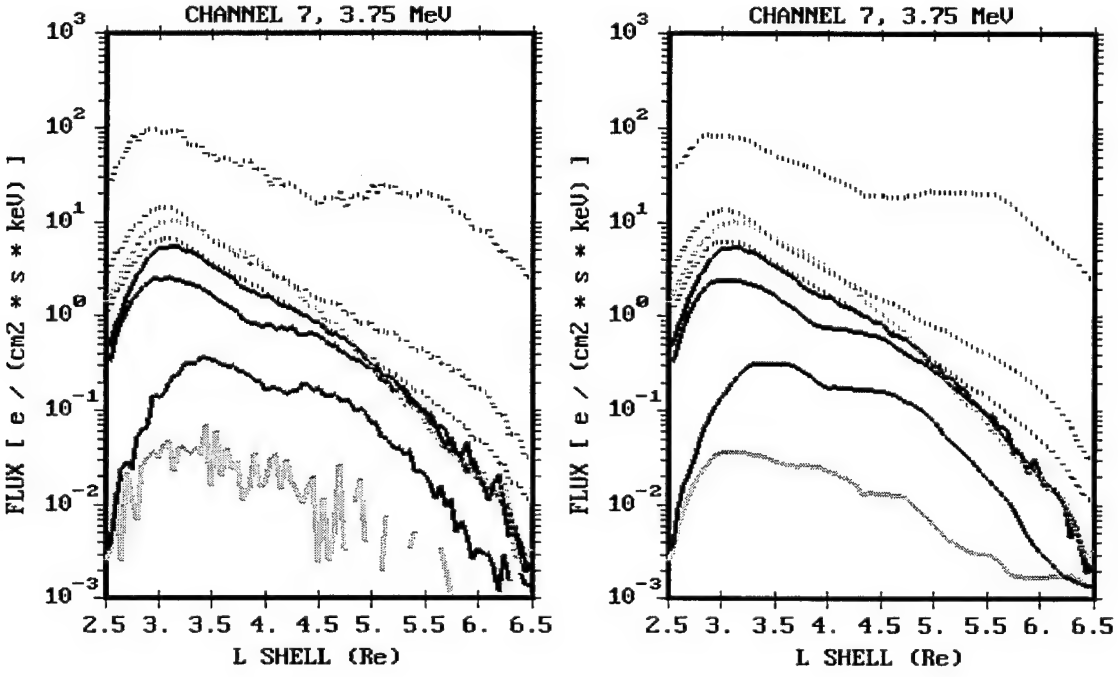

Figure G2. Comparison of model flux profiles before (left) and after (right) smoothing.

Appendix H

Equatorial Omnidirectional Flux Model Profiles

Figure H1 displays the six CRRES_Ap models for each of the 10 energies. Plotted are equatorial omni-directional fluxes vs L. The lowest five energies (from 0.65 to 2.35 MeV) are displayed in Figure H1a, and the highest five energies (from 2.75 to 5.75 MeV) in Figure H1b. The legend to the various curves in each plot is given in the lower right hand corner. As was pointed out in the report of the preliminary models (Brautigam, et al., 1992), for higher Ap_{15} (stronger magnetic activity) the fluxes increase at all energies, while the flux peak moves to lower L for all but the highest energies.

Following the same format as Figure H1, Figure H2 displays the CRRES_AVE and CRRES_MAX models, along with the NASA solar maximum electron model (AE8MAX, which is not distributed with CRRESELE). A comparison between the CRRESELE models and AE8MAX may be found in Gussenhoven, et al., 1996.

The spread in the daily average flux profiles, from which the individual CRRESELE models are constructed, is illustrated in Figure H3. Each plot shows the superposition of all the daily average omnidirectional flux profiles (equatorial) that were averaged together to yield a given CRRESELE model for a given energy channel. The lower left panel is that superposition for the 1.60 MeV channel for CRRES_AVE, and includes all 402 profiles over the entire mission. It shows a spread of up to 5 orders of magnitude for L=3.0-3.5. The top two panels show cases for the 1.60 MeV channel also, but for CRRES_Ap model 1 (left panel, $7.5 < Ap_{15} < 10$) and model 4 (right panel, $20 < Ap_{15} < 25$). The average flux CRRES_Ap profiles corresponding to these two plots are seen in Figure H1a (upper right hand panel). The amount of spread in these two models is typically between 2-3 orders of magnitude - certainly an improvement over the CRRES_AVE model. Although far from perfect, ordering the daily flux profiles by Ap_{15} does provide a better representation of the radiation belt environment. The lower right panel in Figure H3 shows the case for the 0.65 MeV energy channel for CRRES_Ap model 4

($20 < Ap_{15} < 25$). A spread of 4-5 orders of magnitude is seen for L=2.5-3, but only 1-2 orders of magnitude elsewhere. At this energy, electrons are relatively easily injected into lower Ls where they are quickly removed by wave-particle interactions, thus making this regime difficult to model with Ap_{15}.

Despite the inherent difficulties of modeling such a dynamic environment with a single activity index (such as Ap_{15}), there have been some encouraging results in comparing the environment inferred by the CRRES_Ap models (and the Ap_{15} database) and that inferred by DMSP/J4 background measurements for the year 1994. The background counts measured by the Defense Meteorological Satellite Program (DMSP) J4 detector (designed to separately measure 30 eV to 30 keV electrons and ions) correspond to 2 to 3 MeV electrons (Mullen and Holeman, 1994). Since DMSP is in a low altitude polar orbit, the daily averaged background measurements are projected along a model magnetic field back to the magnetic equator (and binned by L), where they can then be compared to the CRRES_Ap equatorial profiles. The Ap database is obtained for 1994 (NOAA's *Preliminary Reports and Forecast of Solar Geophysical Data*) and the Ap index converted to Ap_{15}. For each day of 1994, the equivalent DMSP/J4 equatorial profile is compared to one of the six 2.0 MeV CRRES_Ap model profiles which is selected based on that day's Ap_{15} value. Figure H4 shows the results of this comparison. All three panels share the same x-axis scale of day number of 1994. The top two panels show flux (gray scale) for L vs day. The top panel is the environment inferred by the CRRES_Ap models, and the middle panel is the projected DMSP/J4 background counts. The DMSP/J4 data is truncated at L=5 because the region beyond that maps back to the auroral oval where the signal from lower energy electrons becomes dominant. The bottom panel is the Ap_{15} index vs day. Since the CRRES_Ap models (top panel) are in flux units and the DMSP/J4 data is in count rate, a quantitative comparison cannot be made. However, there is quite good qualitative agreement in that the periodic (27 day period) enhancements, as well as the quiet period, seen in the DMSP/J4 data, are both reflected in the top panel.

Thus, we are encouraged by the capabilities of CRRESELE, and yet also realize the need for a more extended electron radiation belt flux database. With a greater understanding of the mechanisms driving the dynamics, and a larger data set spanning a complete solar cycle, we will be in a much better position to predict the extremely variable electron population.

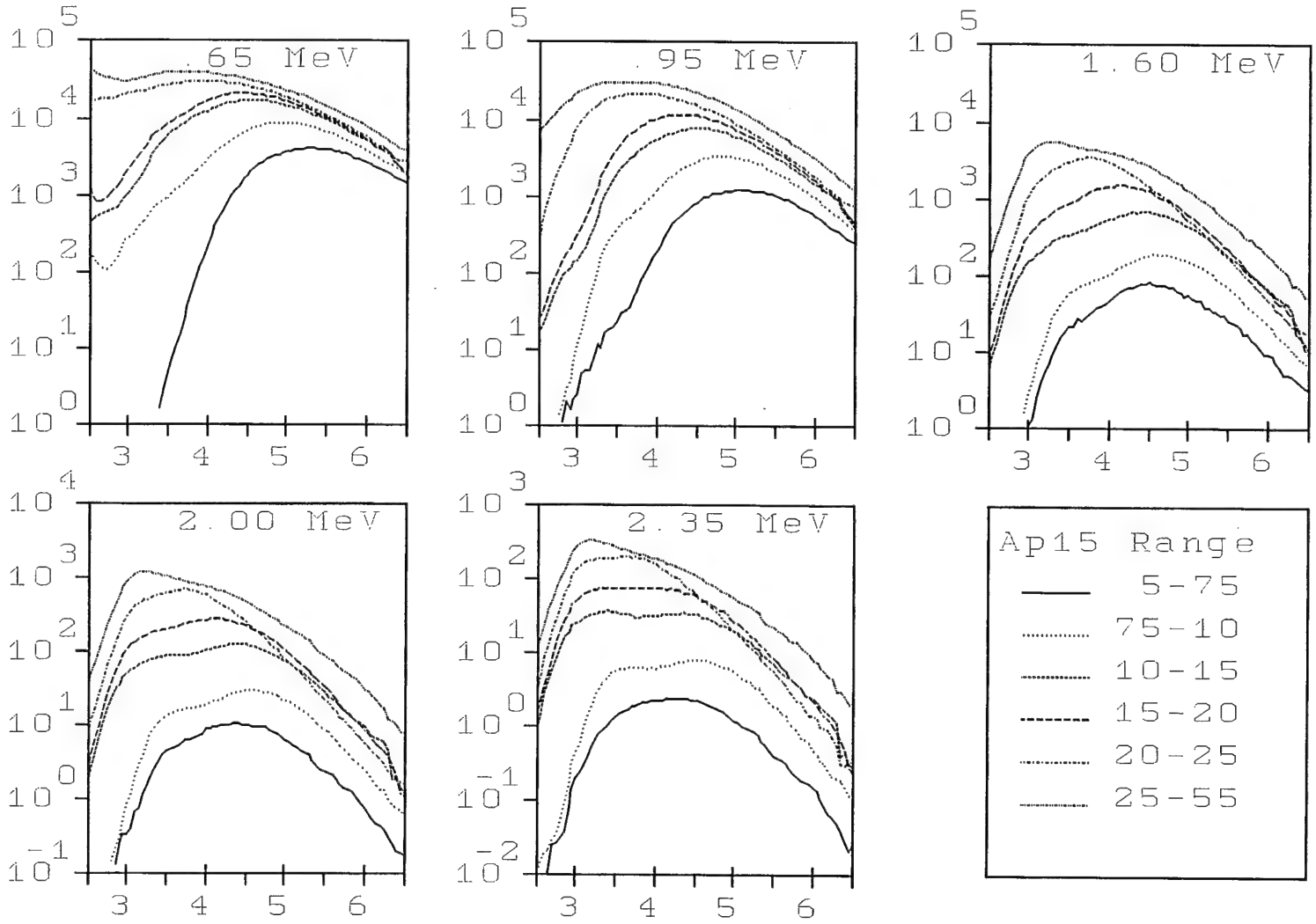

Figure H1a. CRRES_Ap model profiles (legend in lower right panel), plotted as equatorial omnidirectional flux versus L shell for five energies (0.65-2.35 MeV). Flux units are electrons/(cm^2 s keV).

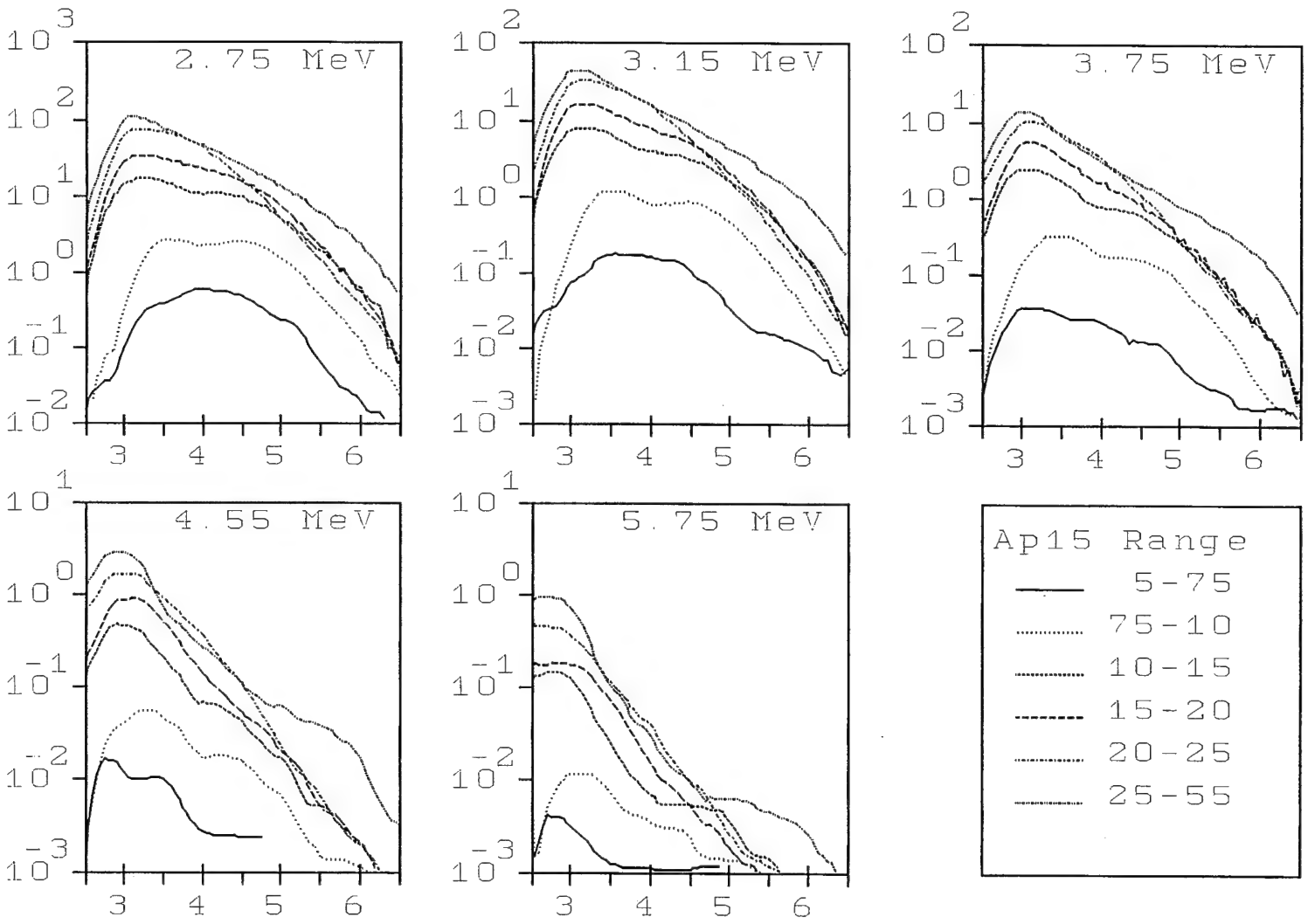

Figure H1b. CRRES_Ap model profiles (legend in lower right panel), plotted as equatorial omnidirectional flux versus L shell for five energies (2.75-5.75 MeV). Flux units are electrons/(cm^2 s keV).

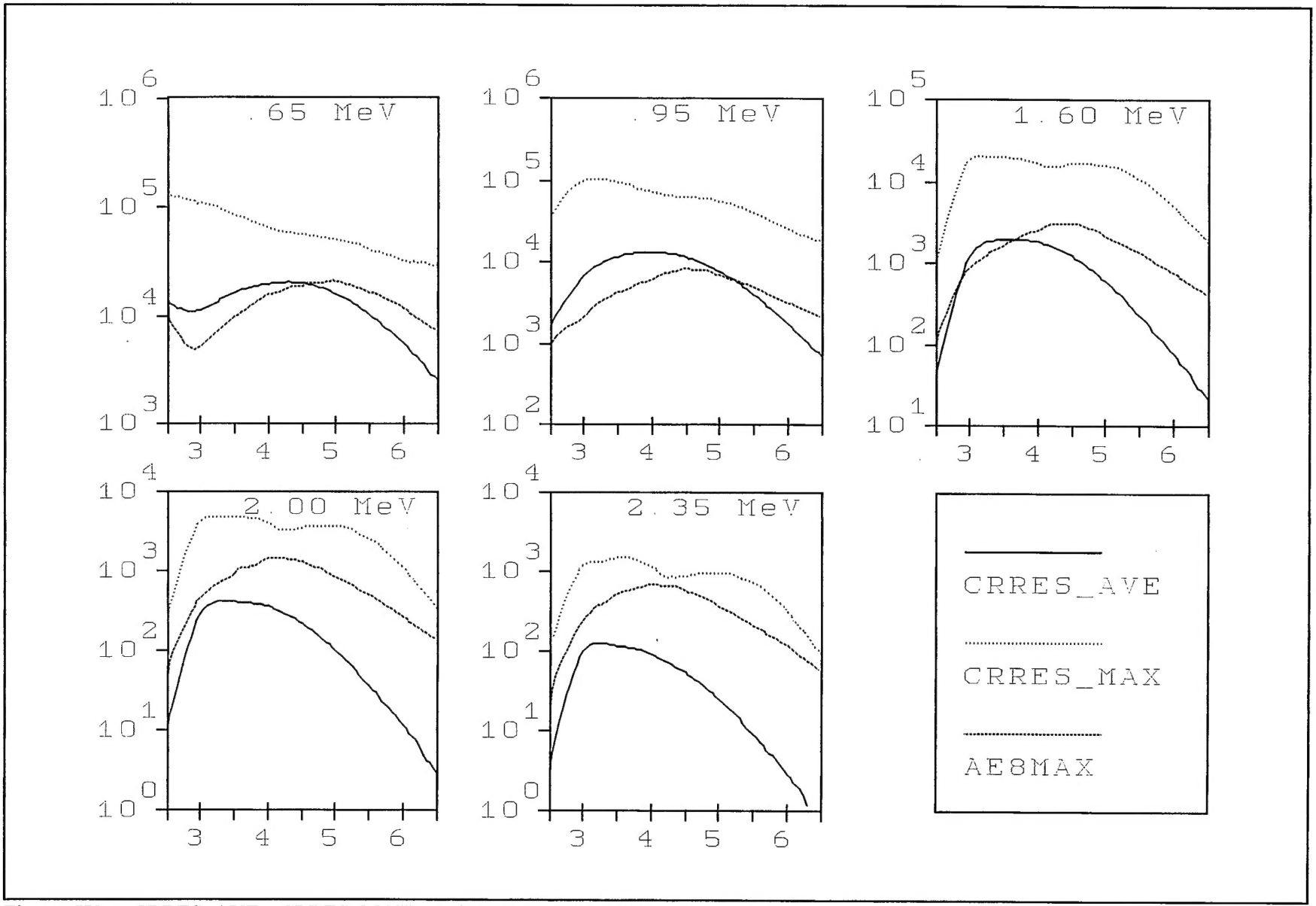

Figure H2a. CRRES_AVE, CRRES_MAX, and NASA AE8MAX model profiles (legend in lower right panel), plotted as equatorial omnidirectional flux versus L shell for five energies (0.65-2.35 MeV). Flux units are electrons/(cm^2 s keV).

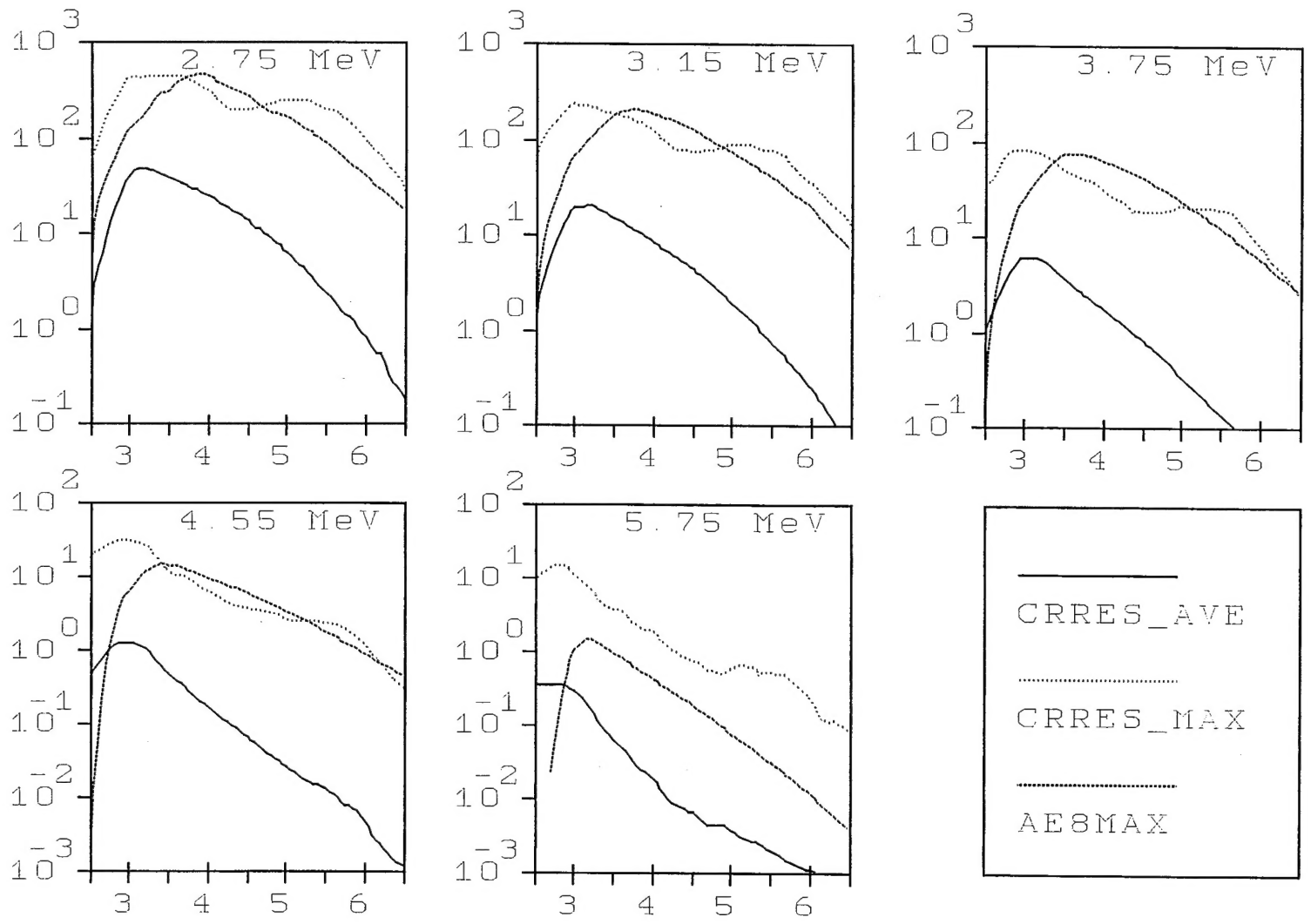

Figure H2b. CRRES_AVE, CRRES_MAX, and NASA AE8MAX model profiles (legend in lower right panel), plotted as equatorial omnidirectional flux versus L shell for five energies (2.75-5.75 MeV). Flux units are electrons/(cm^2 s keV).

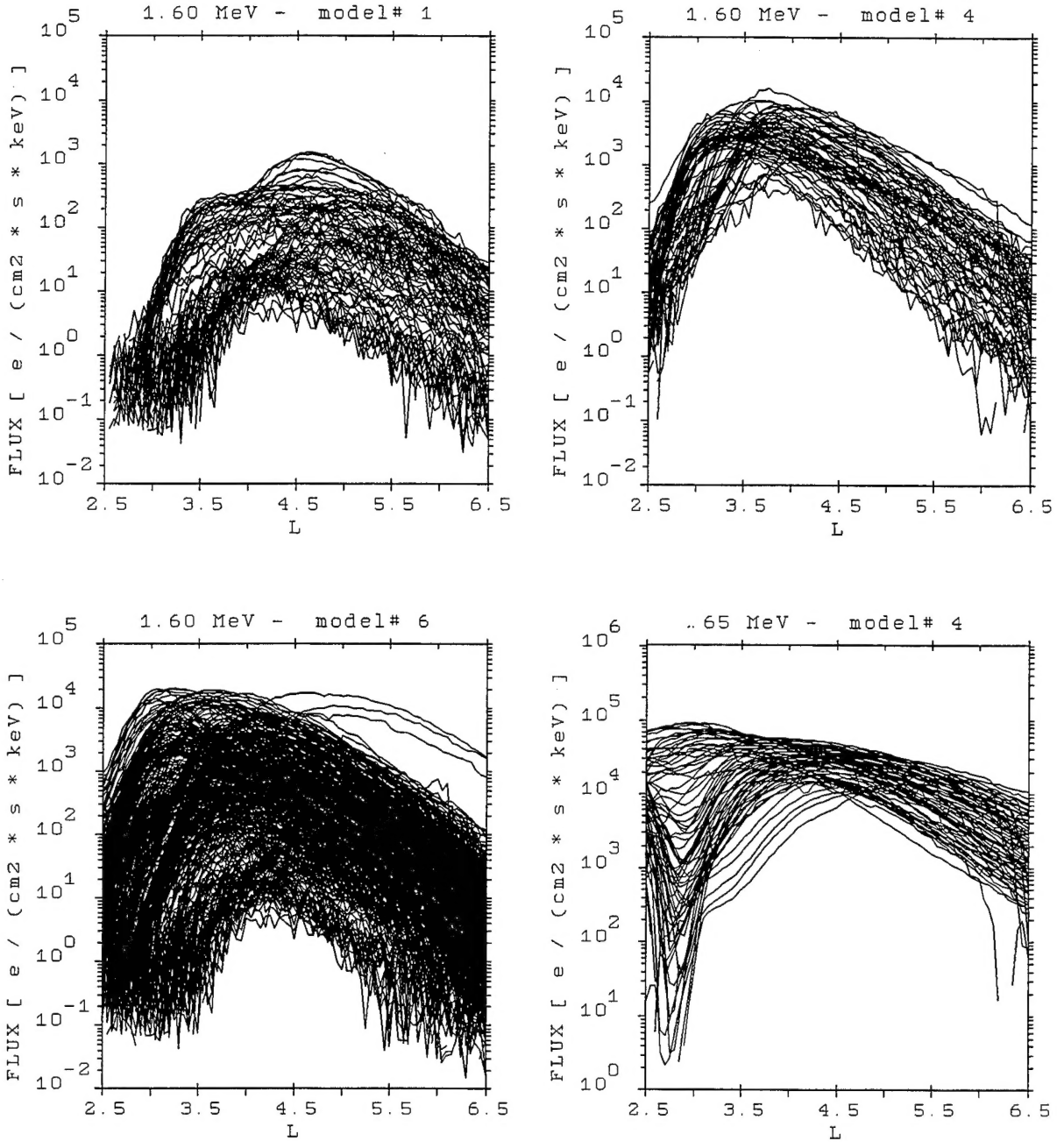

Figure H3. These daily average omnidirectional equatorial profiles illustrate the spread in magnitude of flux which contribute to individual models and channels (as indicated on top of plot panels).

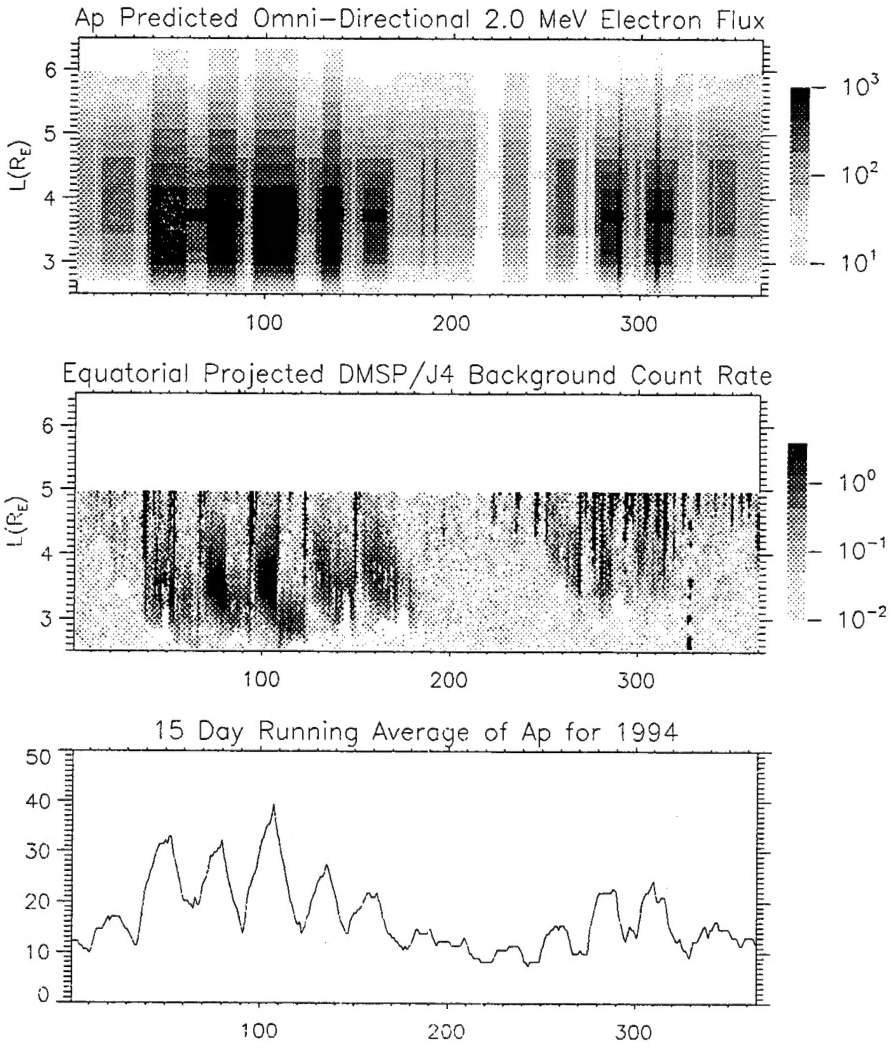

Figure H4. Comparisons between DMSP/J4 equatorial profiles (count rate) and CRRES_Ap predicted equatorial profiles (flux)